

Rochester Institute of Technology

RIT Digital Institutional Repository

Theses

10-1-1987

A mathematical analysis of an electronic dot generating scanner for dot resolution and tone reproduction

Frederick K. Waechter

Follow this and additional works at: <https://repository.rit.edu/theses>

Recommended Citation

Waechter, Frederick K., "A mathematical analysis of an electronic dot generating scanner for dot resolution and tone reproduction" (1987). Thesis. Rochester Institute of Technology. Accessed from

This Thesis is brought to you for free and open access by the RIT Libraries. For more information, please contact repository@rit.edu.

Certificate of Approval -- Master's Thesis

School of Printing and Management Sciences
Rochester Institute of Technology
Rochester, New York

CERTIFICATE OF APPROVAL

MASTER'S THESIS

This is to certify that the Master's Thesis of
Frederick K. Waechter Jr.

With a major in Printing Technology
has been approved by the Thesis Committee as
satisfactory for the thesis requirement for the
Master of Science degree at the convocation of

October, 1987

Thesis Committee: Joseph D. DeLorenzo
Thesis Advisor

Name Illegible
Graduate Program Coordinator

Miles Southworth
Director or Designate

A MATHEMATICAL ANALYSIS OF AN ELECTRONIC
DOT GENERATING SCANNER FOR DOT RESOLUTION
AND TONE REPRODUCTION

by

Frederick K. Waechter Jr.

A thesis submitted in partial fulfillment of the
requirements for the degree of Master of Science in the
School of Printing and Management Sciences in the
College of Graphic Arts and Photography
of the Rochester Institute of Technology

October, 1987

Thesis Advisor: Dr. Joseph D. DeLorenzo

Title of Thesis: A Mathematical Analysis of an Electronic Dot Generating
Scanner For Dot Resolution and Tone Reproduction

I, Frederick K. Waechter Jr., prefer to be contacted each time a commercial
request for reproduction is made.

I can be reached at the following address. 1036 Milne Drive

Lockport , IL, 60441

Ph: (815) 838-1989

Author: Frederick K. Waechter Jr.

Date: 12/12/87

ACKNOWLEDGMENTS

I would like to gratefully acknowledge the many people who made the completion of this thesis possible at Rochester Institute of Technology.

Dr. Joseph D. DeLorenzo, my graduate thesis advisor, who provided the encouragement, motivation and challenges to complete this paper. I want to thank him for his time and the opportunity to work with him.

Dr. Roger L. Easton, for whom without his great persistence and patience the completion of the Fourier Optics portion of this study would not have been possible. Many thanks.

Mr. Joseph L. Noga, for his assistance in the basic understanding of the scanner.

Mr. Michael R. Peres, special thanks for his time and assistance with the microphotography portion of this study.

Mr. Blair Richards, for his help with basic scanner information.

Mr. Jim Hamilton, thanks for his assistance with the black/white contact film printing and processing.

Special thanks to my parents, Fred and Lynne Waechter; Aunt Harriett Layfield; sisters: Joan Cumpston, Jean Waechter, and Jill Arkin; for without their endless patience, support and encouragement this thesis would have never been completed.

TABLE OF CONTENTS

	Page
LIST OF TABLES.....	(v)
LIST OF FIGURES.....	(vi)
ABSTRACT.....	1
 CHAPTER I	
INTRODUCTION	
Electronic Dot Generating Scanners.....	1
 CHAPTER II	
HYPOTHESIS	
Hypothesis.....	2
 CHAPTER III	
METHODOLOGY	
Theoretical.....	3
Experimental.....	3
Equipment.....	4
 CHAPTER IV	
REVIEW OF LITERATURE	
Bellis and Moon.....	5
DeLorenzo and Garsin.....	5
Eastman Kodak Company.....	6
Hecht and Zajal.....	6
Korman.....	7
Linfoot.....	7
Summary.....	7
 CHAPTER V	
FUNCTIONAL DESCRIPTION	
Functional Block Diagram.....	9
Scanner Optics.....	11
Signal Compression.....	14
Gradation Processing.....	15
Color Computer.....	15
Digitization.....	16
Screening Computer.....	16
Film Exposure.....	17
Footnotes.....	18
 CHAPTER VI	
SYSTEM CHARACTERIZATION	
Scanning Spot Optics.....	19

TABLE OF CONTENTS

CHAPTER VI

Primary Color Optics.....	20
Unsharp Masking Optics.....	24
Photomultipliers.....	27
Signal Compression.....	28
Gradation.....	28
Color Computer.....	30
Digitization.....	35
Screening Computer.....	36
Linearization.....	36
Film Exposure and Development.....	38
Summary.....	39
Footnotes.....	41

CHAPTER VII

EXPERIMENTAL RESULTS

Scan Results.....	42
Dot Structure.....	42
Microphotography.....	43

CHAPTER VIII

SUMMARY

Conclusions.....	52
Recommendations for Future Work.....	54

BIBLIOGRAPHY.....	55
-------------------	----

APPENDIX A

Glossary of Terms.....	57
------------------------	----

APPENDIX B

Scanning Procedure and Data.....	60
----------------------------------	----

APPENDIX C

Microphotography Equipment and Procedure.....	63
---	----

APPENDIX D

Microcomputer Equipment and Software.....	65
---	----

APPENDIX E

Fourier Optics.....	77
---------------------	----

APPENDIX F

Digitization Theory.....	93
Footnotes.....	97

LIST OF TABLES

		Page
1	Aperture Data (Drum $\varnothing 212\text{mm}$).....	20
2	Cutoff Frequencies for the Scanning Aperture.....	21
3	Cutoff Frequencies for the Unsharp Masking Annulus.....	24
4	END Values.....	30
5	Cutoff Frequencies for the Calculated Unsharp Masking.....	31
6	Tone Reproduction Data.....	60

LIST OF FIGURES

		Page
1	Functional Block Diagram.....	10
2	Aperture Diagram.....	12
3	Scanning Lens System.....	13
4	Scanning Spot Generation Optics Diagram.....	19
5	Scanning Aperture Optics Diagram.....	20
6	Cylinder Function.....	22
7	Sombrero Function.....	22
8	Aperture Mathematical Analysis.....	22
9	MTF for $a = 33\mu\text{m}$	23
10	Halftone and Isometric for $a = 33\mu\text{m}$	23
11	Unsharp Masking Mathematical Analysis.....	25
12	MTF for $a = 33\mu\text{m}$, $b = 99\mu\text{m}$	26
13	Halftone and Isometric for $a = 33\mu\text{m}$, $b = 99\mu\text{m}$	26
14	Photomultiplier Voltage vs. Input Density.....	27
15	Response of Signal Compression.....	28
16	Voltage Out of Signal Compression.....	29
17	Signal After Tone Reproduction.....	30
18	Unsharp Mathematical Analysis.....	32
19	MTF for $a = 33\mu\text{m}$, $b = 99\mu\text{m}$	32
20	Halftone and Isometric for $a = 33\mu\text{m}$, $b = 99\mu\text{m}$	33
21	Edge Enhancement Mathematical Analysis.....	34
22	Edge Enhancement.....	34
23	Edge Enhancement Input/Output.....	35

LIST OF FIGURES

		Page
24	Digitization Mathematical Analysis.....	35
25	Screening Computer.....	36
26	Percent Dot on Film vs. Density on Film.....	37
27	Exposure Time vs. Density on Film.....	38
28	Film Development Mathematical Analysis.....	39
29	% Dot on Film vs. Density.....	42
30	URGA Resolution Wedge.....	43
31	Microphotography: Parallel Solid Line (0°) Input.....	45
32	Microphotography: Parallel Solid Line (0°) Output.....	45
33	Microphotography: 45° Solid Line Input.....	46
34	Microphotography: 45° Solid Line Output.....	46
35	Microphotography: Perpendicular Solid Line (90°) Input.....	47
36	Microphotography: Perpendicular Solid Line (90°) Output.....	47
37	Microphotography: Solid Patch Input.....	48
38	Microphotography: Solid Patch Output.....	48
39	Microphotography: 60% Dot Input.....	49
40	Microphotography: 60% Dot Output.....	49
41	Microphotography: 30% Dot Input.....	50
42	Microphotography: 30% Dot Output.....	50
43	Microphotography: 1.20 Output.....	51
44	Microphotography: 1.20 Output.....	51
45	MTF for $a = 43\mu\text{m}$	78
46	Halftone and Isometric for $a = 43\mu\text{m}$	78

LIST OF FIGURES

		Page
47	MTF for $a = 64\mu\text{m}$	79
48	Halftone and Isometric for $a = 64\mu\text{m}$	79
49	MTF for $a = 96\mu\text{m}$	80
50	Halftone and Isometric for $a = 96\mu\text{m}$	80
51	MTF for $a = 130\mu\text{m}$	81
52	Halftone and Isometric for $a = 130\mu\text{m}$	81
53	MTF for $a = 270\mu\text{m}$	82
54	Halftone and Isometric for $a = 270\mu\text{m}$	82
55	MTF for $a = 43\mu\text{m}$, $b = 126\mu\text{m}$	83
56	Halftone and Isometric for $a = 43\mu\text{m}$, $b = 126\mu\text{m}$	83
57	MTF for $a = 64\mu\text{m}$, $b = 192\mu\text{m}$	84
58	Halftone and Isometric for $a = 64\mu\text{m}$, $b = 192\mu\text{m}$	84
59	MTF for $a = 96\mu\text{m}$, $b = 288\mu\text{m}$	85
60	Halftone for $a = 96\mu\text{m}$, $b = 288\mu\text{m}$	85
61	MTF for $a = 130\mu\text{m}$, $b = 390\mu\text{m}$	86
62	Halftone and Isometric for $a = 130\mu\text{m}$, $b = 390\mu\text{m}$	86
63	MTF for $a = 270\mu\text{m}$, $b = 810\mu\text{m}$	87
64	Halftone and Isometric for $a = 270\mu\text{m}$, $b = 810\mu\text{m}$	87
65	MTF for $a = 43\mu\text{m}$, $b = 126\mu\text{m}$	88
66	Halftone and Isometric for $a = 43\mu\text{m}$, $b = 126\mu\text{m}$	88
67	MTF for $a = 64\mu\text{m}$, $b = 192\mu\text{m}$	89
68	Halftone and Isometric for $a = 64\mu\text{m}$, $b = 192\mu\text{m}$	89
69	MTF for $a = 96\mu\text{m}$, $b = 288\mu\text{m}$	90

LIST OF FIGURES

		Page
70	Halftone and Isometric for $a = 96\mu\text{m}$, $b = 288\mu\text{m}$	90
71	MTF for $a = 130\mu\text{m}$, $b = 390\mu\text{m}$	91
72	Halftone and Isometric for $a = 130\mu\text{m}$, $b = 390\mu\text{m}$	91
73	MTF for $a = 270\mu\text{m}$, $b = 810\mu\text{m}$	92
74	Halftone and Isometric for $a = 270\mu\text{m}$, $b = 810\mu\text{m}$	92
75	Analog Input Signal.....	93
76	Sampled Wave.....	93
77	Fourier Transform of $f(t)$	94
78	Square Input Wave.....	94
79	Fourier Transform.....	95

AUTHOR'S STATEMENT

The author has written this paper for an audience with a technical background regarding the design and operation of electronic dot generating scanners. A detailed engineering or imaging science background is not required for readers to understand the material presented in this paper.

A 399ER Hell Graphics scanner is the model for this study. The study is intended to be a general analysis and not specific to the Hell product. The Hell scanner was modeled because of its availability at Rochester Institute of Technology in Rochester, New York.

ABSTRACT

An electronic dot generating scanner is a complex machine. This complexity is based in the photographic methods which the scanner is designed to duplicate. This study addresses the mathematical principles of the entire scanner system. This paper was intended to provide an improved understanding of the scanner system.

The hypothesis states that a mathematical analysis with experimental verification can be developed to accurately model the internal optics, tone reproduction, and output dot characteristics of an electronic dot generating scanner.

The analysis begins with a functional block diagram, which shows the information flow through the scanner. This diagram breaks the process into its smaller components and provides the framework for the mathematical analysis.

The diagram has an accompanying word description for each section of the scanner. The basic function of the scanning optics, data compression, gradation, color correction, digitization, halftone screening, and film exposure is discussed for the scanner system.

The system characterization develops a mathematical analysis based on the functional block diagram. It details the theory behind each section of the scanner. Fourier optics, electrical engineering, and photographic tone reproduction theories are applied to the various scanner functions.

The scanning optical system is analyzed using Fourier transform techniques to describe the effect of the imaging system on image transmission. Modulation Transfer Functions (MTF's) are used to show the output frequency spectrum of the scanning aperture. The electronic unsharp masking is modeled by using an optically equivalent process.

The photomultiplier and associated data compression's effect on the reproduction of shadow detail is demonstrated graphically. The improvement in the photomultiplier response

is noted due to logarithmic compression.

The flexibility of the gradation processing is demonstrated through a graphical representation of the treatment of a typical signal. The gradation selection provides the operator with the ability to tailor the output to the reproduction requirements of each transparency. This flexibility is a great advantage, if properly utilized, because it allows customization of each separation.

The color computer is described in general terms. The subjective manner, which color correction is determined is not addressed in this paper.

Digitization is described with its associated compromises in signal integrity. The sampling and quantization processes are detailed.

The screening computer and linearization together effectively transform a digitized gray level into a dot on film. The linearization sets up the scanner for its processing environment.

The output signal from the screening computer drives a laser modulator, which controls the light traveling through the fiber optic cables to expose the film. The film is developed to produce the final separation.

An experimental tone reproduction curve was produced. The type of curve produced versus the expected is discussed. The input/output characteristics are examined through the scanning of a UGRA resolution wedge. The UGRA wedge input and separation film output is analyzed using microphotographic methods to examine structure.

This hypothesis was not proven because of the many assumptions required by the scope of this project, which made the prediction of overall systems results not possible. Although, each function (minus color correction) of the scanner is analyzed. This model of the entire scanning system from input optics through the final film exposure can be utilized to improve understanding of the entire scanner system.

Chapter I

INTRODUCTION

An electronic dot generating scanner produces four individual color separations from continuous tone color originals. Essentially, the scanner is a large computer programmed to perform tasks once done by skilled craftsmen with process cameras. If properly utilized, this computer has the capacity to produce separations with greater efficiency than those produced by the craftsmen.

There is little technical information published related to the scanner system, and the published material which does exist is confined to certain components of the system. A study of the integrated system would be beneficial to the industry.

The objective of this project was to develop a model that accurately predicts the output dot characteristics and tone reproduction of the scanner. This model details the functional elements of the scanner. The model utilizes Fourier representations of the imaging system and unsharp masking functions. The photomultiplier detection, data compression, gradation, digitization, screening, linearization, and film development are modeled either mathematically or graphically. This method will provide a theoretical model (minus color correction) representing the entire scanner from the imaging system to halftone film output. The complexity of the scanner and availability of the scanner did not make this objective possible.

An experimental tone reproduction curve was generated. A comparison to a theoretical curve was not possible because of the extensive number of assumptions in the theoretical model. These assumptions provide too much variation to present an accurate result. Microphotography was utilized to observe the input/output characteristics of the system.

Chapter II

HYPOTHESIS

A mathematical analysis can be developed and experimentally verified to accurately predict the imaging system, tone reproduction, and output dot characteristics of an electronic dot generating scanner.

Chapter III

METHODOLOGY

Theoretical

The block diagram of the scanner, shown in Figure 1, describes the functional steps from original copy to final film output. A model was developed from the diagram which applies mathematical and graphical functions to describe the scanning optics, photomultiplier response, unsharp masking, tone reproduction, color correction, halftone conversion and output dot structure.

Experimental

An experimental tone reproduction curve was produced. An UGRA resolution wedge was scanned for dot and line resolution. An experiment was performed to determine if the scanner produces the same dot structure for the same input density. The film input and output was analyzed using microphotographic techniques to examine the UGRA dot structures and edges.

Equipment

399 ER Hell Scanner: See Appendix B

Densitometer: X-Rite 309

Film Type: Kodak ES Scanner Film

Film Processor: Kodak Rapid Access

Microphotography: See Appendix C

Microcomputer hardware and software listing: See Appendix D

Transparency: Carbon-dye gray scale and a UGRA resolution wedge

Chapter IV

REVIEW OF LITERATURE

A review follows for Donald C. Bellis, Jr. and James E. Moon's paper given at the 1981 meeting of TAGA and published in the Proceedings of the 1981 Meeting of the Technical Association for the Graphic Arts, pp. 231-250.

A successful data gathering system was described to analyze the interactions of a typical electronic scanner. The discussion concentrates on the problems related to spectral response (photomultipliers), color control and film/scanner interface. The paper contains graphs of photomultiplier, color computer output and film/scanner output response. These graphs demonstrate the weakness of the photomultiplier response to small shadow changes, color computer voltage modification and density responses of various Kodak films to specific wavelengths of light. Also, there is a discussion of the differences between the scanner's spectral response and a human vision system.

A review follows for the article by J.D. DeLorenzo and P.A. Garsin entitled "Image Shaping In Nonlinear Xerographic Systems", presented at the Fourth International Conference on Electrophotography in Washington, D.C. in November of 1981.

The physical characteristics of the Xerographic process are modeled using mathematical methods. The paper breaks down the process into five areas. Optics, photoreception, development, toner transfer, and toner fuser are discussed as they relate to the shape of the final image on paper.

The optical characteristics are described by a transfer function with its related spread

function to show the resolution losses in the optical system. The photoreceptor's frequency independent photodischarge and potential dark decays are modeled to demonstrate the design revisions required to account for these natural decay effects. The development function is linearly formalized to a transfer function and associated spread function with appropriate constants to adjust for the design variables. The transfer of toner is represented by a normalized transfer function and its inverse Fourier transform. This function describes the toner dispersion during transfer. The fuser is characterized by a frequency independent nonlinear function that maps the mass profile into optical density on the copy.

The above functions are applied to system responses from wide to narrow lines and fine line sharpening. These functions are an excellent model of the actual experimental results.

A review follows for the publication by the Eastman Kodak Company entitled "The Color-Separation Scanner - Q-78," 1981.

The publication discusses the history of scanners, types of scanners available, important scanner components, photographic principles, original copy, scanner output, and quality control standards. There is a brief description of each topic which presents the general idea of the task for each section of the scanner as it relates to the process camera. The booklet is a general information publication to assist understanding the new technology.

A review follows for the book by Eugene Hecht and Alfred Zajac entitled "Optics."

The book gives an excellent description of Fourier Optics. Fourier Optics are used to evaluate optical imaging systems in terms of spatial frequencies. It discusses one-dimensional and two-dimensional Fourier transforms, linear systems, convolution theory, and modulation transfer functions. These concepts are applied to model the imaging

system of the scanner.

A review follows for the article entitled "Accuracy Of Color Reproduction with the Digital Computer - Scanner System of Color Separation" by N.I. Korman given at the 1972 meeting of TAGA and published in the Proceedings of the 1972 Meeting of the Technical Association for the Graphic Arts, pp. 156-166.

The article describes the color array used to determine dot sizes in the screening computer. The potential solutions and problems of using this type of array are presented. Also, colorimetric matching's practicality is discussed.

The internal accuracy of the halftone conversion "look up" tables was questioned in the article. The electronic conversion of the process causes the majority of the errors. A graphical representation shows this error can be significant, but proper steps can be taken to limit the effect.

A review follows for the book by E.H. Linfoot, Fourier Methods of Optical Image Evaluation.

This book discusses optical system image evaluation and comparisons which are made by taking the modulation transfer function (MTF) of each system. The MTF is the evaluation tool of the reproduction system's capabilities.

Summary

The Bellis and Moon paper outlined an analysis methodology and the information flow thru a scanner. It described the equipment used to monitor the scanners response to a controlled input. This input was electronically generated and not film based. This method

would be the most accurate and was not possible under the conditions at the school. Kodak purchased a scanner to do the experimentation for this project. The project took about three years and the majority of the time the scanner was non-functional. Mr. Bellis was very helpful in advising where the possible problems might be found.

The DeLorenzo and Garsin article showed that a complex system could be broken down into a series of mathematical representations. A transfer function for each step was generated. The analysis was based on a large data base of test results to show the interactions. My thesis project did not have this large data base which made the analysis more difficult.

The Optics text provided the background necessary to perform the Fourier analysis. It described why Fourier analysis is the only method used to predict optical system response. The scanner optics were modeled using this theory base.

The Korman article brought out the errors created by transforming a film based into a computer based process. The compromises and human judgement used in this conversion were discussed. This process creates various errors which a complete analysis of the system would account. The limited electrical access made verification of these claims not possible.

These articles and books provided the basis for my paper. They provided valuable insight into the process being analyzed. The optical system analysis would not have been possible without this information.

Chapter V

FUNCTIONAL DESCRIPTION

Functional Block Diagram

The information flow through an electronic dot generating scanner is shown in Figure 1 on the following page. The diagram maps the processes required for an electrically generated color separation. The scanning process is the electronic equivalent to the direct screen method of color separation. Instead of relying on human subjective judgement, a computer algorithm was created to model and perform the process.

The scanner consists of the following functional elements: scanner optics, input transparency, photomultiplier detectors, signal compression electronics, gradation/tone reproduction, color computer, digitization, screening computer, film exposure, and final separation. These elements are discussed in detail in the remainder of this chapter.

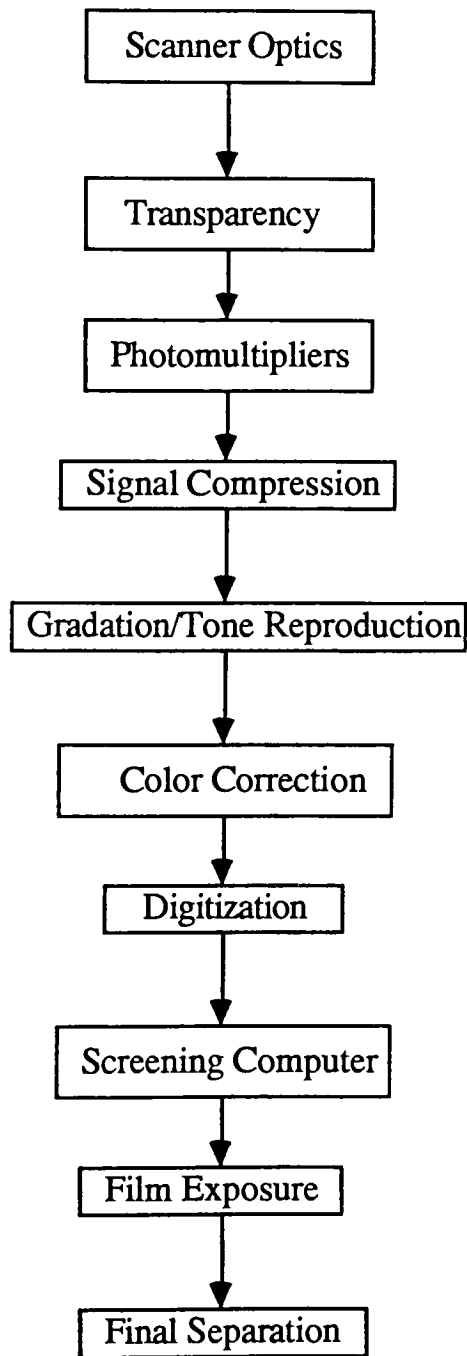


Figure 1. Functional Block Diagram

Scanner Optics

The scanning optics focus light into a beam whose intensity is modulated by the input transparency. The detected intensity is a function of the initial illumination intensity, spot size, and the transmittance or reflectance of the input.

The characteristics of the scanning optics can be analyzed by the point spread function (psf) or by an Optical Transfer Function (OTF). These functions are related by a Fourier transform. The Fourier transform process converts a function from coordinate space (x,y) to the spatial frequency (wavelength) domain, which provides a common basis for the analysis of optical systems. The OTF is in frequency space, whereas the psf is in coordinate space.

The OTF defines the range of spatial frequencies transmitted by this system. The absolute value of the OTF is the Modulation Transfer Function (MTF), which is the function used to discuss the frequency spectrum of incoherent optical systems. The width of the frequency spectrum will provide the detail about the quality of image reproduction possible by the system. The wider the spectrum the more spatial frequencies passed, and the better the image quality.

The point spread function of the scanner is the diameter of the scanning spot, and the OTF is the Fourier transform of the scanning spot - sombrero function. The sombrero function is a oscillatory symmetrical Bessel function, which models the diffraction (spreading) characteristics of light. The Fourier transform process converts a function from coordinate space (x,y) to the spatial frequency (wavelength) domain, which provides a common basis for the analysis of optical systems. This general analysis is applied to the optical system characteristics of the scanner.

The scanning spot is circular and optically adjustable in size. The size is dependent on the enlargement or reduction and screen ruling used for reproducing the original image.

Figure 3 shows the optical system after the scanning drum. The reflected or transmitted light is captured by the scanning lens and focused on the system aperture, which is an annulus (See Figure 2). The annulus is transmissive in the center with a reflective outer ring. The system apertures analyzed were circular, although other geometries are available. The aperture (inside diameter) and annulus are both modeled by cylinder functions, which is the mathematical formula for a uniform circular disk of light.

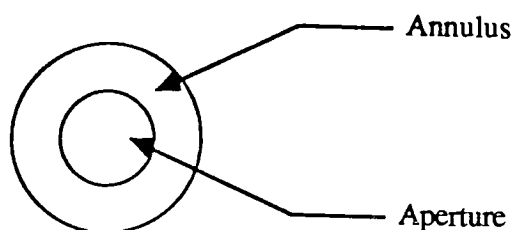


Figure 2. Scanning Aperture

The OTF of the aperture is analyzed by calculating the Fourier transform of the cylinder function. The annulus is calculated by taking the difference of the Fourier transforms of the cylinder functions of the annulus (outside diameter) and aperture (inside diameter). The absolute value of these OTF's (MTF's) were plotted to give the frequency spectrum to the photomultipliers. This frequency spectrum does not account for the effects of various filters applied over the photomultipliers. The lack of specific information on the filters made this assumption necessary.

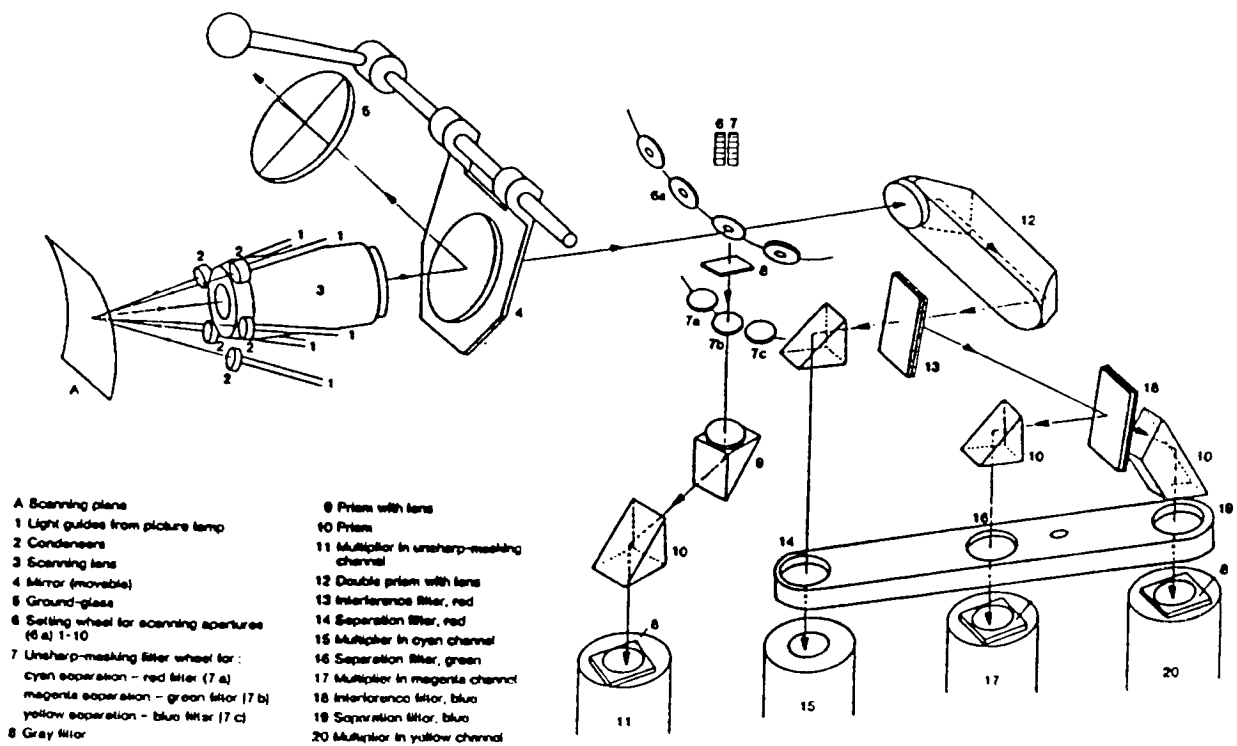


Figure 3. Scanning Lens System¹

The photomultiplier responds to light energy from the imaging system by converting radiant energy to an output voltage. The ability of the photomultipliers to detect small energy changes over the entire tonal range is vital, but the ability of the photomultiplier to differentiate between density levels decreases as density increases. At higher density levels (lower transmitted brightnesses), the photomultiplier signal response flattens.² Therefore, differences between the various degrees of shadows become lost in electrical noise, which means they cannot be retrieved by any method. This limits the reproduction of the fine shadow detail present in most transparencies.

The scanner has four photomultipliers (PMT's), three of which are filtered to detect the amount of cyan, magenta, and yellow dye in each pixel. The signal from the fourth

photomultiplier is used for unsharp masking (edge enhancement). The creation of the black printer is discussed in the color correction section of Chapter VI.

The photomultiplier voltages are processed separately for each color. The fourth PMT produces the unsharp masking signal, whose filter is chosen by the operator. Normally, the green filter (magenta channel) is used because human vision is more sensitive to edges in this portion of the visible spectrum. The edge enhancement is calculated by taking the normalized value of the voltage difference between the main (aperture) and unsharp masking (annulus) signals and adding it back to the main voltage. The normalization ensures that there is no edge enhancement in a uniform area (i.e. the voltage difference is set to zero at a solid). The edge enhancement was modeled in an optically equivalent manner. The Fourier transform of the elements was substituted for the voltages with an identical result.

Unsharp masking enhances the output edge information. The degree of edge enhancement is determined by the relative diameters of the aperture and annulus. The larger the ratio of outer to inner annular diameter, the greater the enhancement. The required annulus size is related to the amount of information required by the system. The enlargement or reduction and screen ruling of a reproduction determine the information requirement. The scanning system requires more information (samples) to produce an enlargement than a reduction because the data is being expanded. If there is not sufficient data, the picture will have poor continuity.

Signal Compression

The output voltage of the photomultiplier is modified logarithmically to improve the deficiencies in the photomultiplier response and more closely model the human vision

system. The signal is compressed less in the shadows (low voltage) than in the highlights (high voltage). Also, this compression forces all signals to lie within a specific voltage range and introduces additional electrical noise (error) to the system. The effect is to provide proportionally more quantization (gray) levels at lower signal levels.³

Gradation Processing

After compression, the output signal is split, with half demodulated to compute the unsharp masking and half kept intact for gradation processing in the tone reproduction computer.

The tone reproduction voltage is split into fifths, thus allowing for better control of the highlight, quarter-tone, mid-tone, three-quarter tone, and shadow areas of the reproduction. Each of the five signals is applied to a separate nonlinear amplifier and the summed result can create virtually any curve shape required for the proper tone reproduction.

Color Computer

The color computer corrects for hue errors in the inks (gray balance), calculates the black printer, applies gray component replacement (GCR), and undercolor removal (UCR). These adjustments are set by the operator based on image type and printing conditions.

The Equivalent Neutral Density (END) values assign a certain dot size for the three primary colors to a particular density to achieve proper gray balance. These values allow adjustment for hue error due to imperfect absorption of the cyan ink by reducing the size of the magenta dot where both magenta and cyan dots. Similarly, the END values allow

reduction of the yellow dot where both yellow and magenta occur to account for the imperfect absorption of the magenta ink.

GCR replaces the unnecessary (darkening) percentage of the third color in a three-color dot overlap by black throughout an entire picture. UCR replaces a percentage of the three color dot overlap by black in the shadows of a transparency. Both GCR and UCR reduce printing ink costs and improve ink trapping conditions, but involve subjective judgment and are not addressed in this paper.

Digitization

Digitization transforms an analog signal into a digital signal. The analog voltage is sampled at the Nyquist frequency ($1/2B$, where B = signal bandwidth) to maintain signal integrity. If the ability to sample and maintain signal integrity was not possible this process would fail because of too much data. The Nyquist frequencies validity is derived in Appendix F.

This sampled data is quantized, where a binary number is assigned to each individual signal level in the available dynamic range. The dynamic range is typically 0-255. Each number corresponds to an available gray level. The quantization process introduces unavoidable rounding error into the system.⁴

Screening Computer

The screening computer converts the digitized gray level signal to a voltage to drive the exposure modulator, while accounting for the particular screen ruling, enlargement or reduction, and dot shape specified by the operator. The screen angle, which is aligning the halftone dots at angles to one another, is necessary to avoid a moire pattern. This

distracting pattern will occur at any out of register point when trying to print dot on dot (same screen angle). The typical screen angles used on electronic dot generating scanner are 45° black, 75° magenta, 90° yellow, and 105° cyan.

The shape of the output dots can be varied from round to elliptical. The enlargement or reduction is provided by storing each gray level pixel. This gray level data file is sampled at a predetermined rate to produce the required enlargement or reduction.

A separate linearization process specifies the Density versus log E (exposure) curve for the current scanner and processing conditions. This linearization provides the "lookup" table for the screening computer which converts the gray level to the proper exposure voltage (time) to drive the laser modulator.

Film Exposure

The screening computer signal drives a laser exposure modulator, which controls the exposure time. The exposure is performed by fiber-optic cables, which produce micro-dots on the film. The actual micro-dots are circular in shape and small enough to require multiples to create each halftone dot. The number of fiber optic cables activated for each dot controls the shape. The positioning of the fiber optic cables will determine the possible dot shapes from a given scanner.

The rapid access film used has certain advantages in development time and temperature required over lith film. These factors make the film easier to use in a production atmosphere.

FOOTNOTES

¹Hell Graphics Corp., Hell DC300 Operators Manual: 19.

²Bellis Jr., Donald C. & Moon, James E., "Technical Analysis of Electronic Color Scanners: Theory, Applications, and Techniques." Proceedings of the Technical Association of the Graphic Arts, 1981: 231-250.

³Schwartz, Mischa, Information, Transmission, Modulation and Noise. New York: McGraw-Hill Book Company, 1980: 117.

⁴Ibid.

Chapter VI

SYSTEM CHARACTERIZATION

Scanning Spot Optics

The scanning spot is created by the system shown in block diagram form in Figure 4. The optical condenser and lens focus the illumination, which is then directed by a mirror onto the transparency. The scanning spot diameter used provides the best available resolution for an ideal system with no diffraction losses. The scanning spot diameter is adjustable from $20\mu\text{m}$ to $270\mu\text{m}$ according to a manufacturer supplied graph. However, tests showed that the $50\mu\text{m}$ setting corresponds to an actual spot size of $7\mu\text{m}$ to $10\mu\text{m}$. Thus, there must be a 7:1 optical reducer in the system. The actual spot size on the transparency ranges from $3\mu\text{m}$ to $90\mu\text{m}$.

The system bandwidth, which describes the rate of change in the spatial frequency distribution passed to the image, is equal to the velocity across the transparency divided by the diameter of the spot ($B = v/d$). The velocity of the drum remains constant, so the spot size determines the system bandwidth. In effect, the spot is rastering the image onto the photomultiplier.

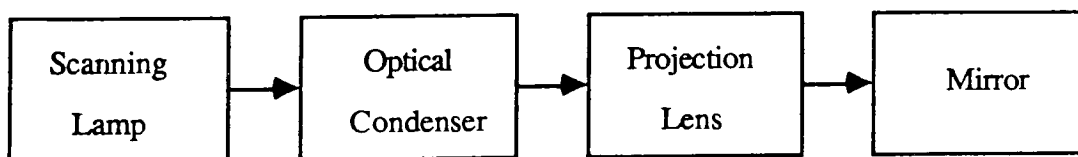


Figure 4. Scanning Spot Generation Optics Diagram

Primary Color Optics

A block diagram of the scanning aperture optical system is shown in Figure 5. The scanning lens collects the light beam transmitted by the transparency onto the annular beam divider, which is transmissive in the center (a) with a reflective outer ring (b). The circular apertures available for the Hell 399ER are listed in Table 1¹. The light beam is split and filtered in red, green, and blue for the primary colors.

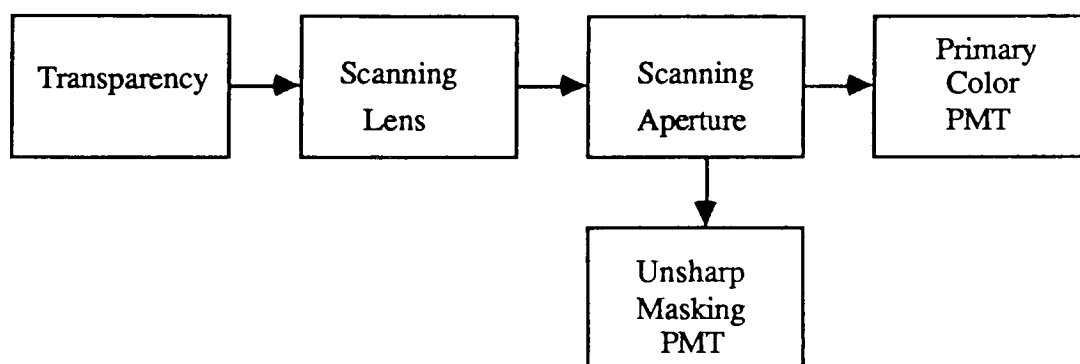


Figure 5. Scanning Aperture Optics Diagram

Number	Scan Aperture (a) (μm)	Unsharp Annulus (b) (μm)	Screen Ruling (lines/in)	Percent Enlargement (%)
1	33	99	150	700
2	43	126	150	420
4	64	192	150	250
5	96	288	150	120
7	130	390	150	70
9	270	810	150	10

Table 1. Scanning Aperture Data (Drum $\phi 212\text{mm}$)

Because the scanning spot is small, the aperture MTF is broad, i.e. many spatial frequencies are passed to the image. With a larger aperture, more image information is

averaged at each pixel, thus the image blurs and detail is lost. As a result, the MTF will become thinner (narrower bandwidth). Graphs of the MTF for each aperture differ only in scale because the ratio of aperture and annulus diameters does not change.

The limiting value of the MTF is the cutoff frequency, i.e. the location of the first zero amplitude on the graph. These are listed in Table 2. The higher the cutoff frequency, the more fine detail is transmitted. Thus, Aperture 1 would have the best detail reproduction. Immediately beyond the cutoff frequency, the image contrast is reversed. This portion of the graph can be misleading because of the absolute value used to calculate the MTF. Actually, the OTF in this area is negative which leads to the contrast reversal. The cutoff frequency range is a function of the aperture diameter and the number of samples used to calculate the MTF. A sample calculation of the cutoff frequency range is shown in Appendix E.

Number	Aperture (μm)	Cutoff Frequency (cycles/mm)
1	33	34.2
2	43	25.3
4	64	17.8
5	96	12.2
7	130	8.4
9	270	4.7

Table 2. Cutoff Frequencies for the Scanning Aperture

Figure 10 is a halftone representation of the MTF amplitude, where bright areas correspond to good response and dark areas to poor response. The amplitude is much greater in the center of the distribution and decreases at higher spatial frequencies.

The isometric display in Figure 10 shows the frequency distribution of the OTF function in two dimensions. The sinusoidal action of the Bessel function is clearly displayed in the isometric plot.

The following mathematical analysis (Figures 6, 7, and 8) and graph (Figure 9) are representations of the Fourier characteristics for the aperture sizes (a). The MTF graphs, halftones, and isometric plots for aperture's 2, 4, 5, 7, and 9 are shown in Appendix E.

$$cyl\left[\frac{r}{2R}\right] = \begin{cases} 1 & \text{for } |r| < R \\ 0 & \text{for } |r| > R \end{cases}$$

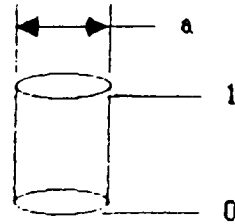


Figure 6. Cylinder Function

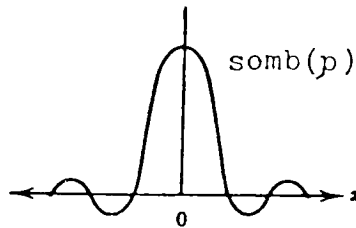


Figure 7. Sombrero Function

$$\mathcal{F}_2\left\{cyl\left[\frac{r}{a}\right]\right\} = a^2 \text{somb}(ap) \equiv \frac{a^2\pi}{4} \frac{2J_1\left[\frac{\pi r}{a}\right]}{\frac{\pi r}{a}} = OTF_{\text{aperture}}$$

$$MTF = |OTF|$$

r = radius vector

a = diameter of scan aperture

$cyl\left[\frac{r}{a}\right]$ = transmittance function of circular aperture

\mathcal{F}_2 = two-dimensional Fourier transform operator

$\text{somb}(ap)$ = *sombrero*, circularly symmetric version of *sinc* function (also called the *Besinc* function)

OTF \equiv optical transfer function

MTF \equiv modulation transfer function

Figure 8. Aperture Mathematical Analysis

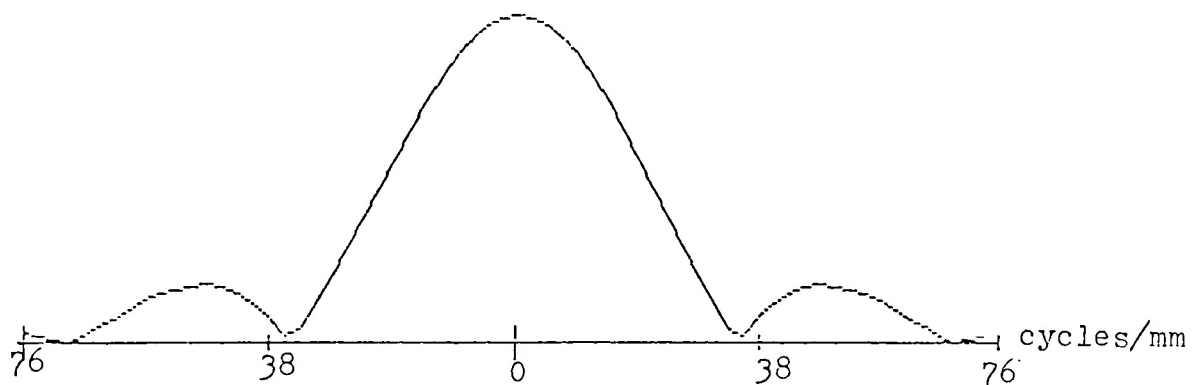


Figure 9. MTF for $a = 33\mu\text{m}$.

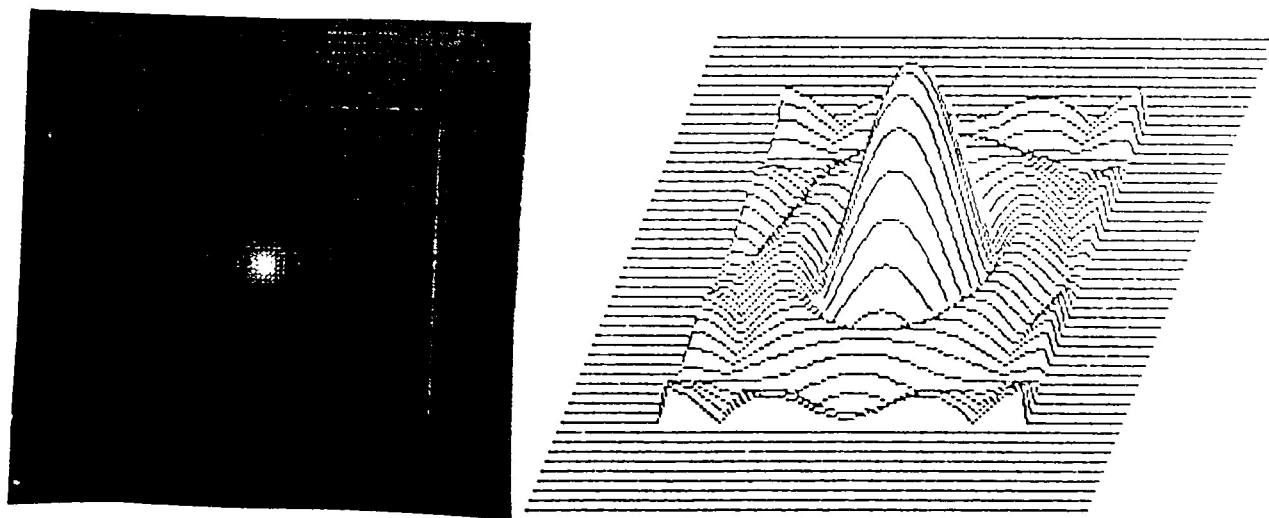


Figure 10. Half-tone and Isometric for $a = 33\mu\text{m}$.

Unsharp Masking Optics

The optics for the unsharp masking consists of a lens system and an adjustable aperture (See Figure 5). The diameter of the annulus determines the enhancement of the edge detected by the system. A green filter is placed over the unsharp masking photomultiplier because studies show human vision is more sensitive to the green portion of the spectrum.²

The unsharp MTF has a much narrower bandwidth than the scanning aperture. This narrow band is more sensitive to transparency density changes than the broader main signal. As before, the graphs are identical in shape because of the ratio of outside to inside diameter has remained constant. The cutoff frequency ranges are listed in Table 3. Aperture 1 detects higher frequency signals and will produce better edge enhancement.

Number	Aperture (μm)	Annulus(μm)	Cutoff Frequency (cycles/mm)
1	33	99	14.2
2	43	126	9.1
4	64	192	5.9
5	96	288	4.7
7	130	390	2.8
9	270	810	1.7

Table 3. Cutoff Frequencies for Unsharp Masking

The halftone and isometric in Figure 13 show the spatial frequency distribution for the masking optics. The following mathematical analysis (Figure 11) and graph (Figure 12) represent this portion of the system. The MTF graphs, halftones, and isometrics for annulus's 2, 4, 5, 7, and 9 are shown in Appendix E.

$$f_{an}(r) = cyl\left[\frac{r}{b}\right] - cyl\left[\frac{r}{a}\right]$$

$$\mathcal{F}_x\left\{cyl\left[\frac{r}{b}\right] - cyl\left[\frac{r}{a}\right]\right\} = F_{an}(\rho)$$

$$F_{an}(\rho) = \left[\frac{b^2\pi}{4} \frac{2J_1\left[\frac{\pi r}{b}\right]}{\frac{\pi r}{b}} \right] - \left[\frac{a^2\pi}{4} \frac{2J_1\left[\frac{\pi r}{a}\right]}{\frac{\pi r}{a}} \right]$$

$$F_{an}(\rho) = OTF_{annulus}$$

$$MTF = |OTF|$$

Figure 11. Unsharp Masking Mathematical Analysis

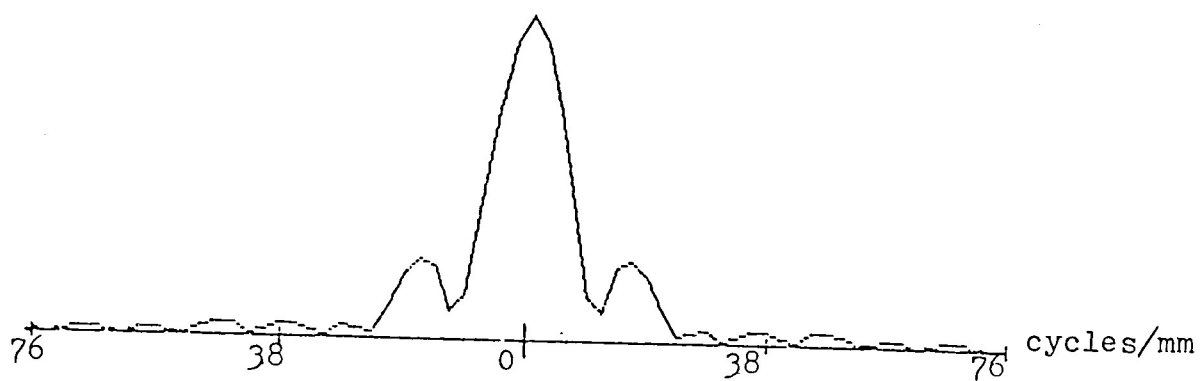


Figure 12. MTF for $a = 33\mu\text{m}$, $b = 99\mu\text{m}$.

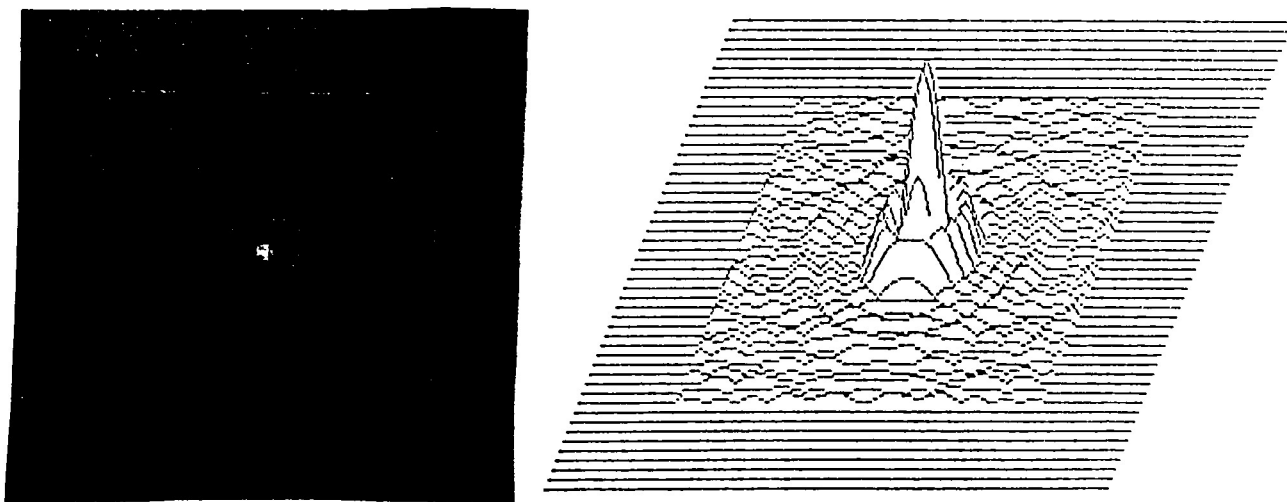


Figure 13. Halftone and Isometric for $a = 33\mu\text{m}$, $b = 99\mu\text{m}$.

Photomultipliers

The nonlinear response of the photomultiplier is given in Figure 14. As the input density increases, the response of the PMT decreases. The response begins to flatten out at a density of approximately 1.75. In general, transparencies will contain detail beyond this point (i.e. in shadows), which will not be detected. This data was gathered from a Hell DC 300 scanner. The new photomultiplier technology produces a better response, but the problem still exists. The testing of the Hell 399ER response would have required some disassembly of the scanner and a block of time not available. All the following voltage output curves are normalized because of this lack of specific information pertaining to each component.

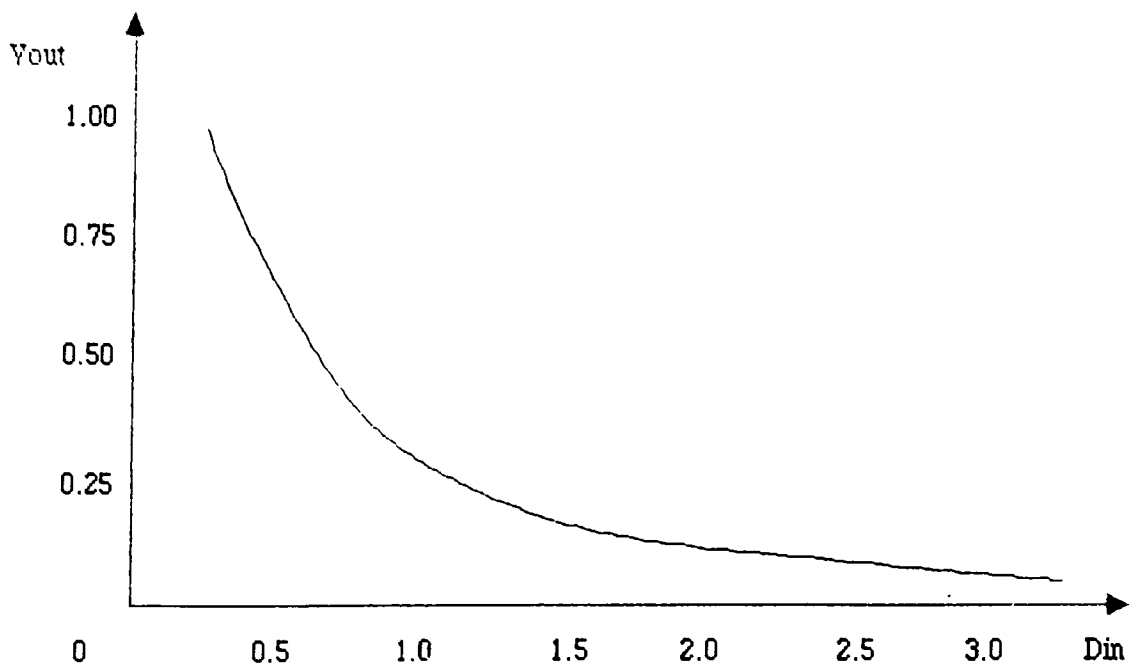


Figure 14. Photomultiplier Voltage vs. Input Density³

Signal Compression

The logarithmic signal compression adjusts the output signal to account for the nonlinear PMT response.⁴ The compression compensates for the PMT's deficiency in detecting differences at higher densities. It improves the density response by approximately 0.5.⁵ Also, the compression introduces noise into the system which cannot be eliminated. This logarithmic relationship is shown in Figure 15.

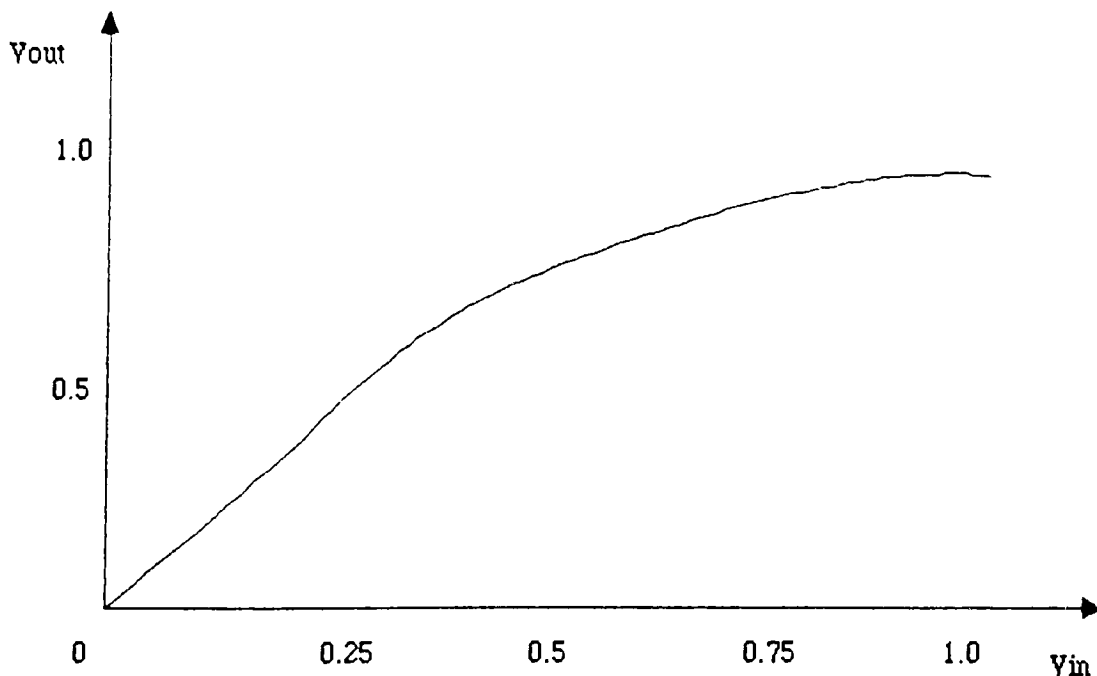


Figure 15. Response of Signal Compression

Gradation

The gradation system is often described as tone reproduction. The scanner has many different tone reproduction curves available for various types of transparencies and picture

content (high, normal and low key images). The high, normal and low key description is the placement of the detail in the picture. A high key image has the important detail in the highlights. A normal key image has both important highlight and shadow detail. A low key image has detail in the shadows. The same gradation curve (3) was used during the experimentation to limit the variables. Curve 3 is used with normal key images. The following Figures 16 and 17 show a typical tone reproduction signal manipulation. The solid horizontal lines represents the ranges for the five nonlinear amplifiers.

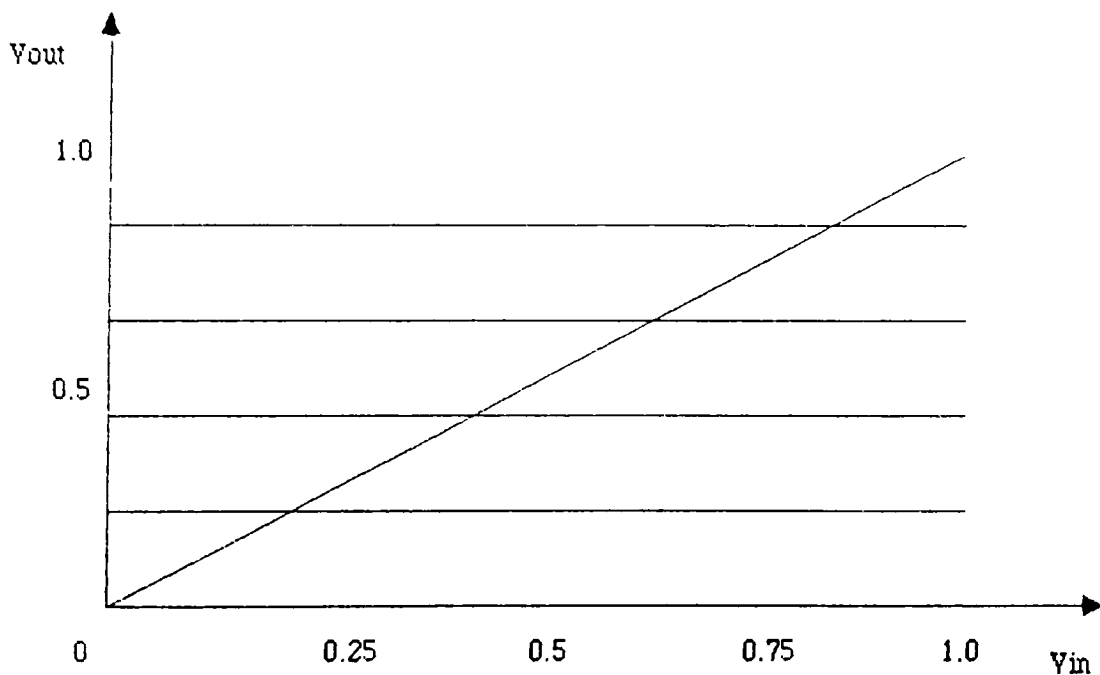


Figure 16. Signal Out of Compression Circuit

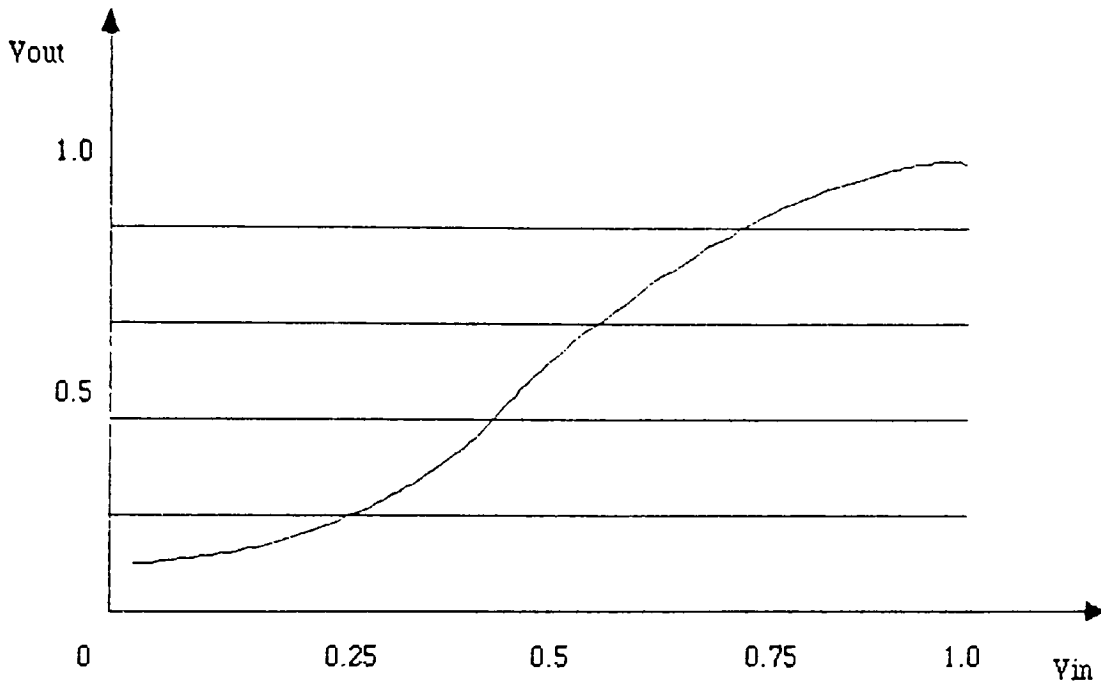


Figure 17. Signal After Tone Reproduction

Color Computer

Color correction is implemented in the color computer. The END values, black printer, UCR, GCR, and unsharp masking are calculated in this section.

A typical set of END values is shown in Table 4. These values will produce gray balance with most transparencies and inks.

Type	Cyan	Magenta	Yellow
Highlight	6	4	4
Middletone	65	50	50
Shadow	95	85	85

Table 4. END Values⁶

The black printer has two different configurations. It can be either a skelton black, which starts at the midpoint (50% dot) of the tone reproduction curve, or a full black, which is the entire curve. The black printer is generated by comparing levels of gray and is

closely related to the amount of UCR being applied. If a high percentage of UCR is applied and the black is not adjusted. The black printer will muddy the shadows of the separation.

UCR and GCR both entail personal judgement as to the percentage required. This subjective judgement determines the proper percentage removed from each type of picture. The subjectivity makes this area very difficult to analyze.

Unsharp masking is modeled as the optical equivalent of the electrical process carried out in the scanner. The MTF's in Figure 19 are representative of the electrical signals. The result is a MTF with edge enhancement. In Figure 22, the edge enhancement is shown by the peak of the MTF at a spatial frequency above 0.

As before, the graphs are identical in shape because the ratio of outside to inside diameter remains 3:1. The cutoff frequencies are shown in Table 5. Aperture 1 detects higher frequency signals and will produce a sharper edge.

Number	Aperture (μm)	Annulus(μm)	Cutoff Frequency (cycles/mm)
1	33	99	34.2
2	43	126	27.2
4	64	192	17.8
5	96	288	12.2
7	130	390	8.4
9	270	810	4.7

Table 5. Cutoff Frequencies for the Calculated Unsharp Masking

The Figure 20 halftone representation is the frequency amplitude distribution of the MTF. This halftone shows a smaller area and larger intensity than the scanning aperture halftone.

The isometric diagram (Figure 20) demonstrates sharp central peaks with a secondary

contrast reversal, as demonstrated by the following mathematical analysis (Figure 18).

The MTF graphs, halftones, and isometric plots for the unsharp masking calculation aperture settings 2, 4, 5, 7, and 9 are shown in Appendix E.

$$F_{un}(\rho) = 2 F_{ap}(\rho) - F_{an}(\rho)$$

$$F_{un}(\rho) = 2a^2 \text{somb}(a\rho) - b^2 \text{somb}(b\rho)$$

$$= 2 \left[\frac{a^2 \pi}{4} \frac{2J_1\left[\frac{\pi r}{a}\right]}{\frac{\pi r}{a}} \right] - \frac{b^2 \pi}{4} \frac{2J_1\left[\frac{\pi r}{b}\right]}{\frac{\pi r}{b}}$$

$$F_{un}(\rho) = OTF_{unsharp}$$

$$MTF = |OTF_{unsharp}|$$

Figure 18. Unsharp Mathematical Analysis

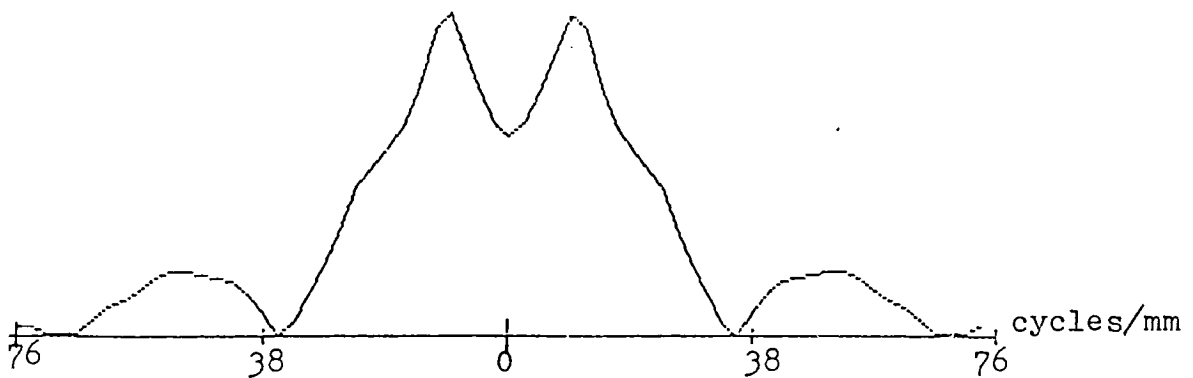


Figure 19. MTF for $a = 33\mu\text{m}$, $b = 99\mu\text{m}$.

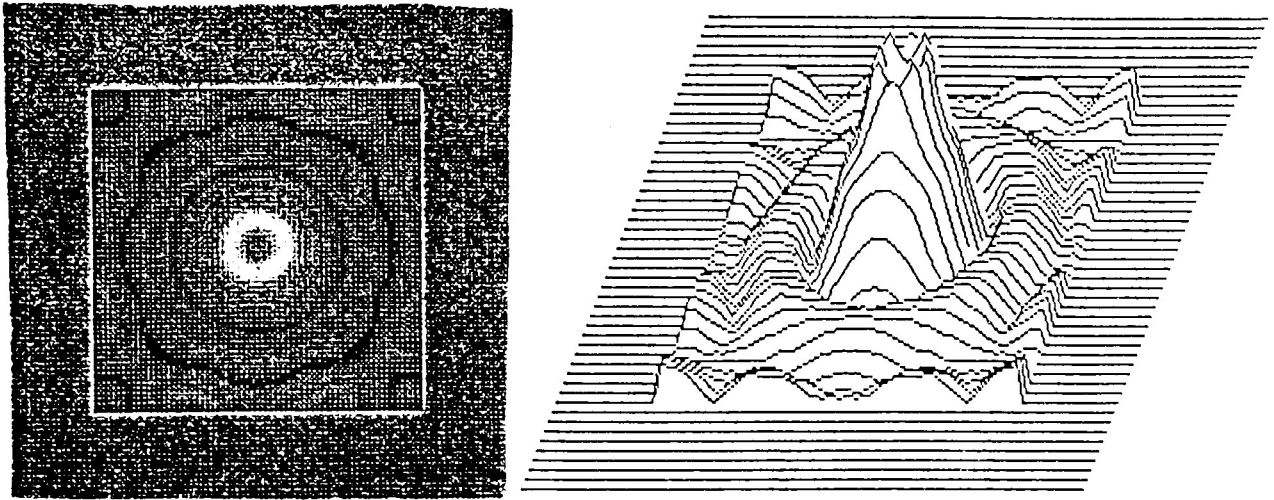


Figure 20. Halftone and Isometric for $a = 33\mu\text{m}$, $b = 99\mu\text{m}$.

An enhanced edge function was modeled as shown in the mathematical analysis (Figure 21). The unsharp masking transfer function was calculated by taking the Fourier transform of the aperture and annulus. The transforms of both functions were normalized, so no enhancement occurred in the large uniform areas. The calculation of twice the resulting aperture MTF minus the annular MTF produced the transfer function. To model an enhanced edge, the system MTF was multiplied by the Fourier transform of the edge function (square wave input), and its inverse transform. The enhanced edge "overshoots" the original edge gray values. The output is shown in Figure 22. The halftone (Figure 23) shows the darkening of the area just before the edge and the lightening just after the edge passes. The graph (Figure 22) and associated halftones (Figure 23) show the imaging systems effect on the output of the scanner.

$f[x,y]$ = edge function

$h_1[x,y]$ = aperture function

$h_2[x,y]$ = annulus function

$$F[\xi,\eta] = \mathcal{F}_2\{f[x,y]\}$$

$$H_1[\xi,\eta] = \mathcal{F}_2\{h_1[x,y]\}$$

$$\hat{H}_1[\xi,\eta] = \frac{H_1[\xi,\eta]}{H_1[0,0]}$$

$$H_2[\xi,\eta] = \mathcal{F}_2\{h_2[x,y]\}$$

$$\hat{H}_2[\xi,\eta] = \frac{H_2[\xi,\eta]}{H_2[0,0]}$$

$\hat{H}[\xi,\eta] = \gamma \hat{H}_1[\xi,\eta] - \hat{H}_2[\xi,\eta]$: transfer function of the scanner

$$\hat{f}[x,y] = \mathcal{F}_2^{-1}\{F[\xi,\eta] \hat{H}[\xi,\eta]\}$$

Figure 21. Edge Mathematical Analysis

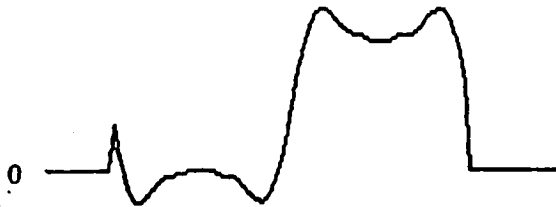


Figure 22. Edge Enhancement

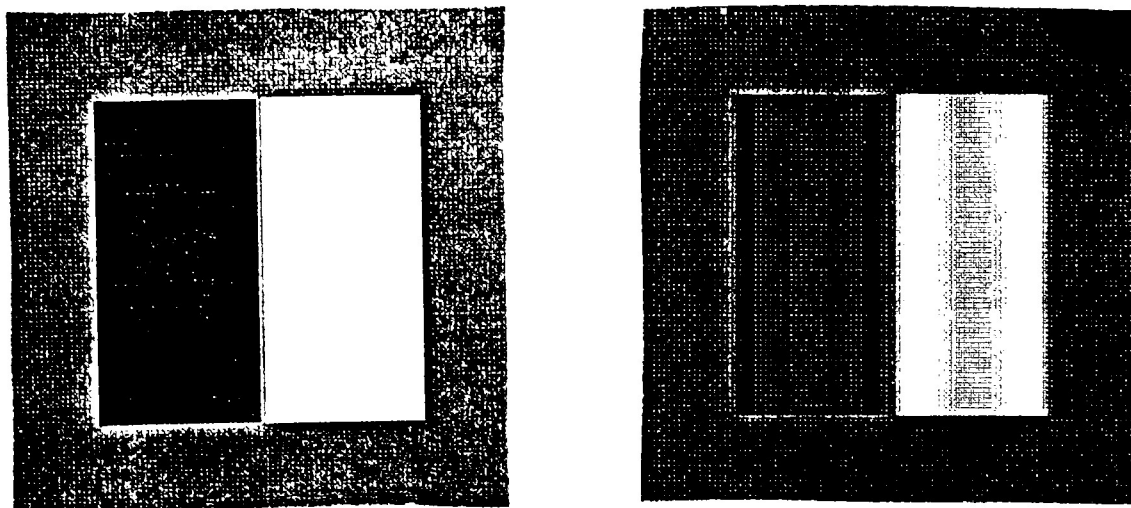


Figure 23. Edge Enhancement Input/Output

Digitization

Digitization process converts an analog signal to discrete values that can be read by a computer. This process consists of sampling and quantization. The digitized data is then assigned to one of 256 gray levels. The following mathematical equation is the general form for signal sampling. A more indepth discussion of digitization process is found in Appendix F.

$$\mathcal{F}_s\{S(t)\} = d F(\omega) + d \sum_{\substack{n=-a \\ n \neq 0}}^a \frac{\sin(n\pi d)}{n\pi d} F(\omega - n\omega_c)$$

n = number of samples

ω = frequency

d = distance between samples

Figure 24. Digitization Mathematical Analysis

Screening Computer

The general function of the screening computer is to convert digital gray levels into corresponding voltages, which represent a percent dot on film. The screening computer enlarges or reduces by changing the sampling frequency. Also, it gives each signal its appropriate screen angle. The screening computer is customized by a "lookup" table test to each particular scanner environment. This screening function is represented by Figure 25.

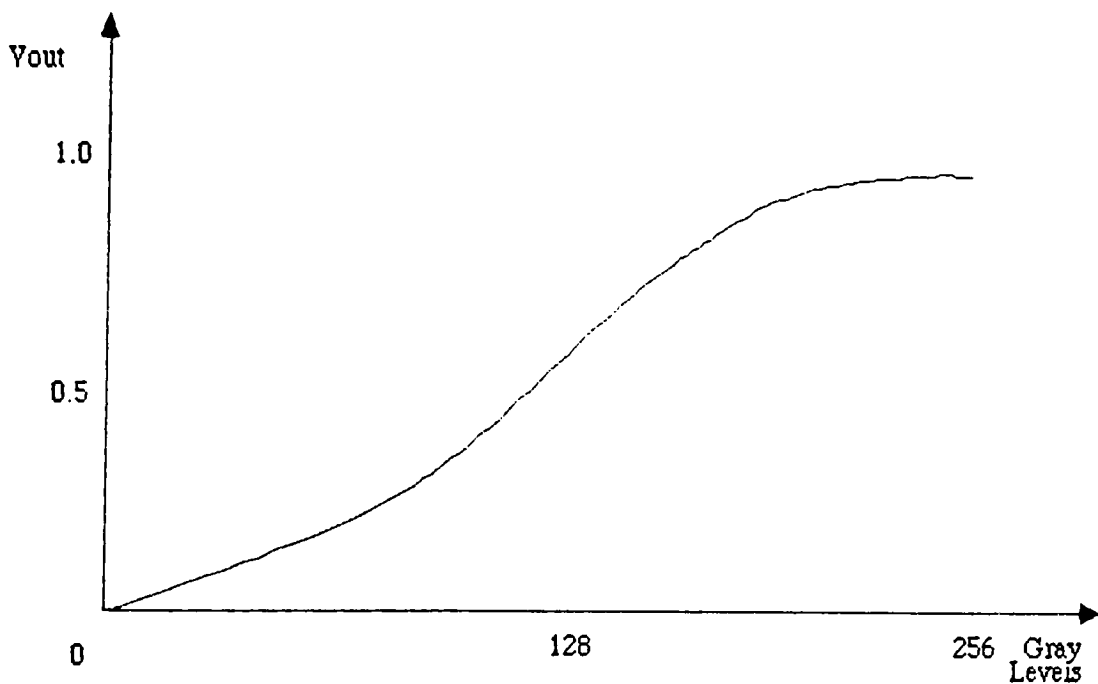


Figure 25. Screening Computer

Linearization

The linearization is performed to bring each scanner into an acceptable operating range for the given production conditions. The information is generated by an internal gray scale. This exposed gray scale film is developed and checked to a standard. If the gray scale is not to the standard, the values can be updated. These internal values provide the

"look up" table used by the screening computer. The following graphs (Figures 26 and 27) are representations of this data.

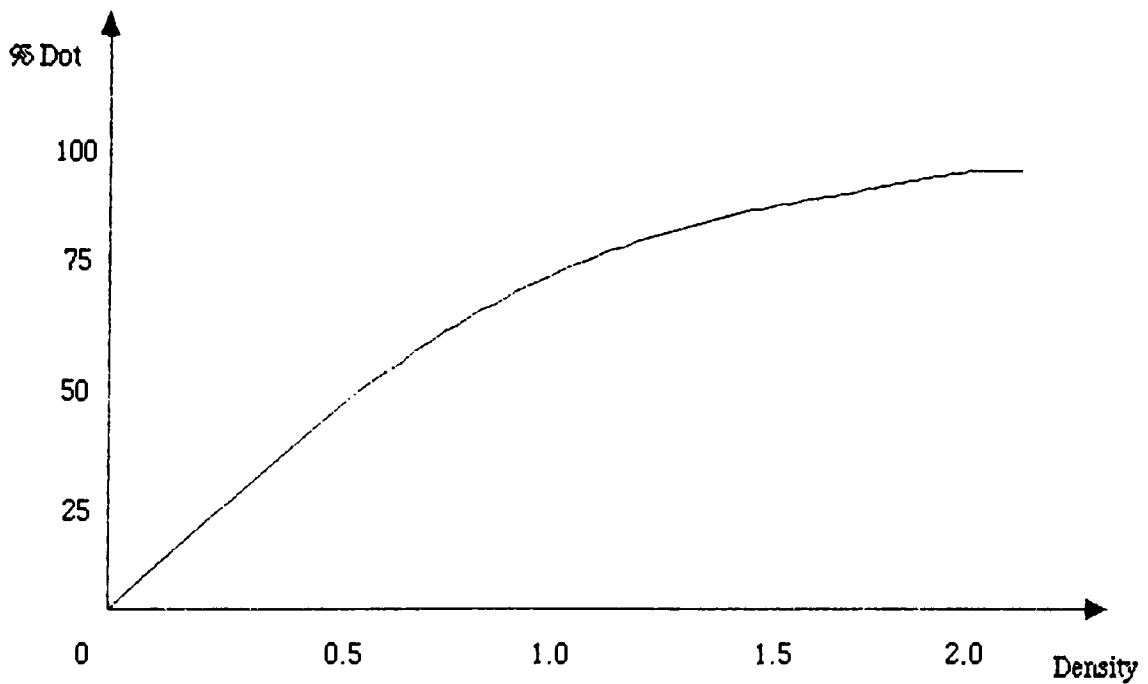


Figure 26. Percent Dot vs. Density on Film

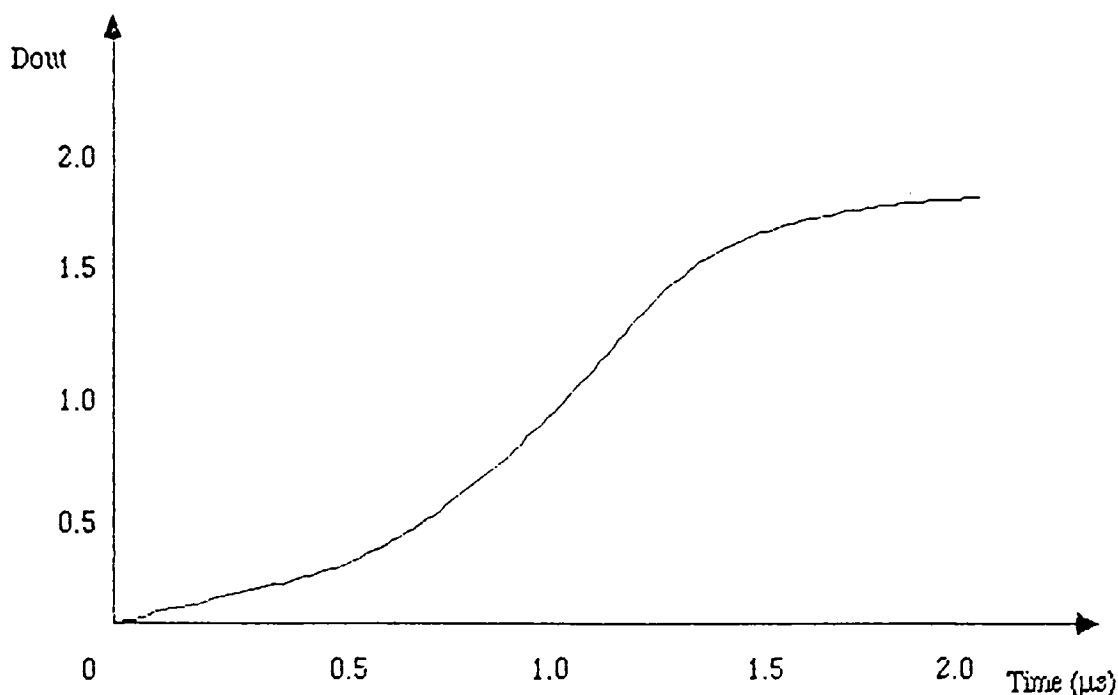


Figure 27. Exposure Time vs. Density on Film

Film Exposure and Development

The film is exposed by an electrical modulator controlling a group of optical fibers. The modulator controls the amount of light and length of time a particular optical fiber will be exposing the film. The fibers produce micro-dots on the film. These dots are circular in shape. The film required for this type of exposure must be very high resolution to utilize the maximum capability of the scanner. The scanner film used for the experimental portion of this study was developed for this type of scanner application.

After exposure, the film is processed. The film development is represented by the following mathematical equation.

$$D = \gamma_n \log E - D_0$$

D_0 = Value at the straight line minus the toe

γ_n = Slope of the straight line

E = Exposure

Figure 28. Film Development Mathematical Analysis

Summary

There are several areas of concern with this theoretical model, which make the calculation of a theoretical tone reproduction and dot characteristics not achievable within the scope of this research. The following assumptions and problems are the reasons for this concern.

First, the model does not address the problem of distortion in the analog electrical signal, which will create processing problems in the scanner. This effect is a major design problem of the scanner electronics. Neglecting this characteristic has introduced significant error into the model, which cannot be ignored. An accurate analysis would require a controlled input and a monitoring of the output to observe the corrections designed into the machine to account for these electrical variations. A test of each area of the scanner would be required.

A more detailed knowledge of each component and its interactions would create a more accurate analysis. This lack of information creates precision problems. Also, each electronic component has a tolerance on its operation, which results in each scanner having to be adjusted for its particular components. Thus, each scanner is different. The scanner would have to be partially disassembled to gather this information and this is not possible given the scanner's role in the school. These two factors are critical to producing a

complete and accurate model.

The color computer has been just described in general terms. An indepth analysis of the system used to apply color correction would make the model more complete. The design of the color computer starts with the Neugebauer equations, but they are severely modified. The strict Neugebauer equations do not work in practice. The Neugebauer equations are adjusted electrically by making all the variables flexible. So, each operator can set the scanner (equaitons) for his conditions. This flexibility and customization would make this model extremely difficult to complete. The development of this model would require significant access to the scanner and may not be possible given the current conditions. It would require a study of the electrical signals passed between the various functions during the color correction phase of the scanning process. Also, the manufacturer's will be very reluctant to provide information on this system for competitive reasons, which will make the study even more difficult.

The dot shape produced is a function of the fiber optic cables and film. A through analysis of the light transmitting capabilities of fiber optic cables and the reaction of the rapid access film to this light would be necessary of create an accurate model of this process. The type of facilities necessary to do this testing are not available.

These restrictions and limitations made the completion of a comprehensive model not possible. Although, this paper is a good framework for a complete analysis.

FOOTNOTES

¹Hell Graphics Corp., Hell 399ER Operators Manual.

²Bellis Jr., Donald C. & Moon, James E., "Technical Analysis of Electronic Color Scanners: Theory, Applications, and Techniques." Proceedings of the Technical Association of the Graphic Arts, 1981: 231-250.

³Ibid.

⁴Ibid.

⁵Ibid.

⁶Southworth, Miles, Color Separation Techniques. 1979: 129.

Chapter VII

EXPERIMENTAL RESULTS

Scanning Results

The following tone reproduction curve was generated from the procedure and data outlined in Appendix B. The experimentation coincided with the development of the theoretical model. Thus, the data will be represented without a comparison for the reasons previously stated. The result obtained was expected considering the normal key gradation curve of 3 and black output channel were used. The mid-tone to highlight range is approximately 0.9, which would be normal for this type of transparency.

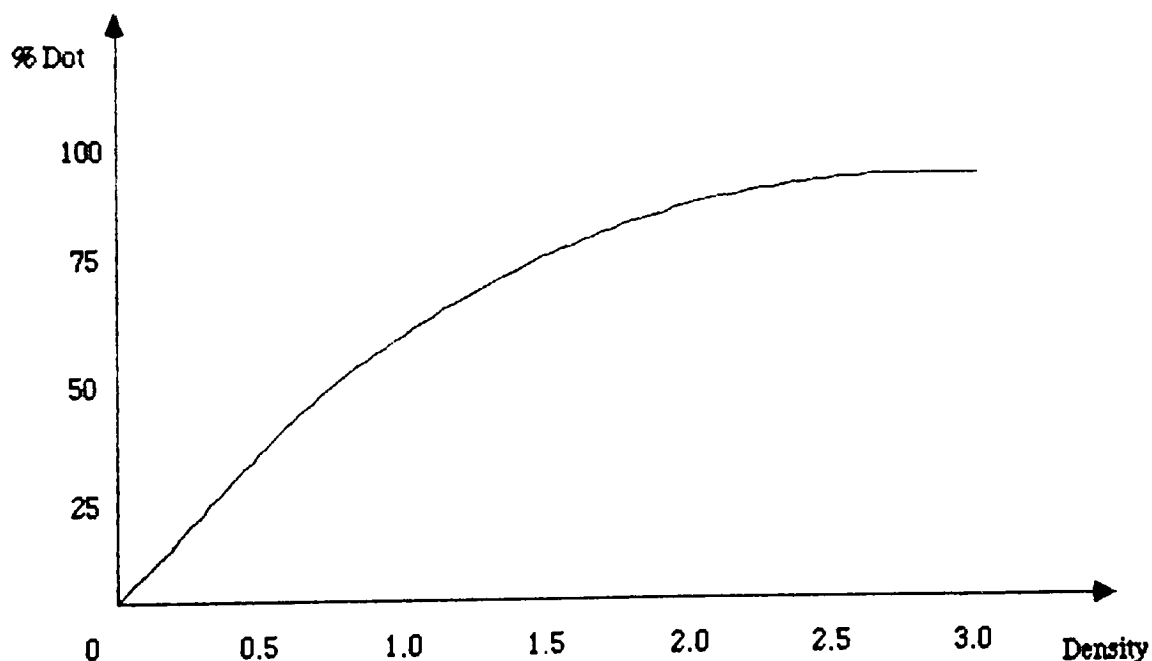


Figure 29. % Dot on Film vs. Density

Dot Structure

The dot structure is demonstrated in the microphotographs by the jagged edges. This

effect is generated by the round micro-dots used to generate the image. These micro-dots give a jagged edge because the circular edge of the micro-dot appears where a straight edge is desired. This variable edge is so small that it is not detectable to the human eye. Thus, the micro-dot technology is acceptable for a scanning system.

Microphotography

Microphotography is used to demonstrate the input/output characteristics of the scanner. It details the transformation from transparency (input) to separation (output). The UGRA wedge shown in Figure 30 (input) was photographed at same size. The output was enlarged 300% to produce a resolved line. These resolution problems were a result of screen angle, width of the input line, and moire pattern. The solid line output was examined at same size and 200% enlargement, but both were unacceptable because of severe line breakup. The angles stated for the line photographs are in reference to the scanning direction.



Figure 30. UGRA Resolution Wedge

The solid line output, parallel to scanner drum rotation (Figure 32), photograph shows very poor edge definition. This poor definition is a result the screen angle and halftoning process.

Figures 33 and 34 (45°) show the best input/output line definition, although the edges are still jagged. The imaging system is better able to resolve the angled line than the straight edge because the black printer's screen angle is 45°, which does not break up the

line as severely.

The perpendicular solid line (Figure 36) output has very poor resolution, which is caused by the screen angle and halftone process. This output is of poorer quality than the parallel line, which is caused by the edges relationship to the rotation direction of the drum. The system detects edges better in the around the drum direction.

The solid patch output (Figure 38) has small white dots. These dots were created because of the tone reproduction curve (Gradation 3) . The density of the solid patch was not high enough to be a halftone solid given that curve. The small dots are very jagged, which is again due to the circular shape of the micro-dots.

The 60% dot input (Figure 39) reads 26% on the film output (Figure 40). This reduction is again caused by the tone reproduction curve. The dot formation is very jagged and spotty. The film development could have caused this uneven dot formation.

The 30% dot input (Figure 41) reads 10% on the film output (Figure 42). This output is very spotty and shows a minimal dot formation.

The 1.20 density input in two places on the original produced identical dot output (Figures 43 and 44). This demonstrates the scanner will reproduce the same dot structure for the same density regardless of the position of the density on the drum. This result was expected because of the optical system of the scanner.

Microphotography is an excellent method for analyzing the scanner output. The jagged edges produced by the fiber optic cable microspots become very apparent, although, they are not detectable to the unaided human eye.

These experimental results begin to build the data base, which would be required to develop a complete scanner system transfer equations. The development of these equations will require a further investigation of the electronic portion of the scanner system.



Figure 31. Microphotography: Parallel Solid Line (0°) Input

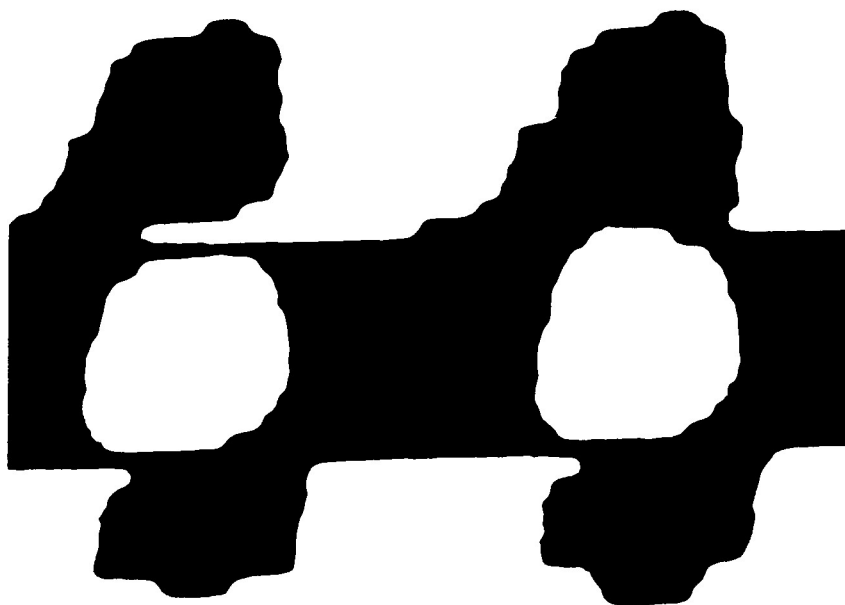


Figure 32. Microphotography: Parallel Solid Line (0°) Output

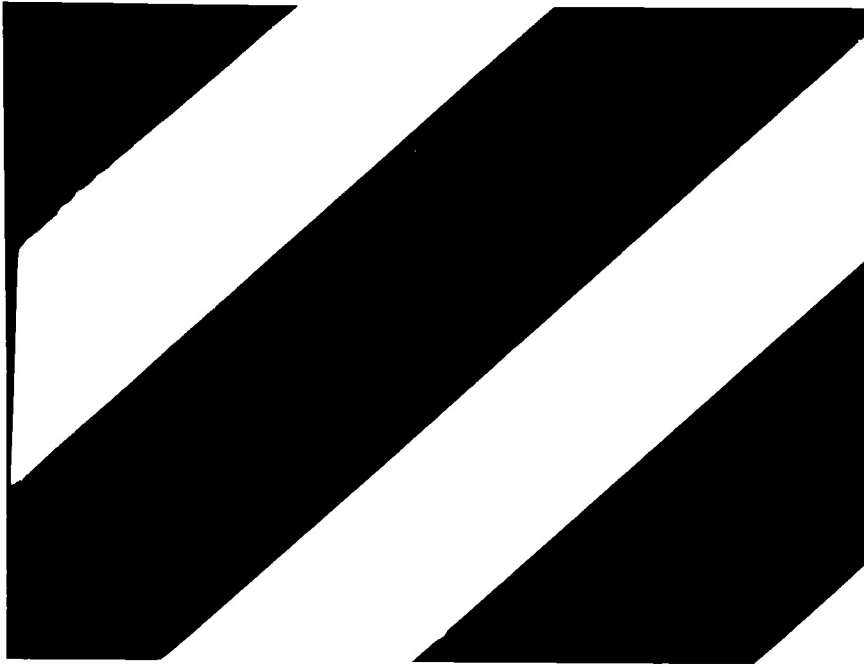


Figure 33. Microphotography: 45° Solid Line Input

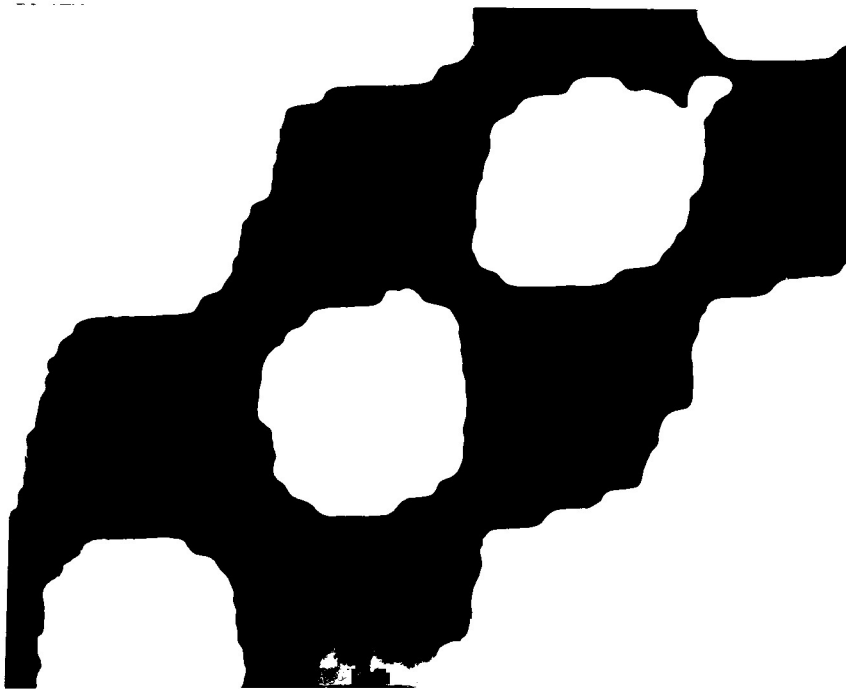


Figure 34. Microphotography: 45° Solid Line Output



Figure 35. Microphotography: Perpendicular Solid Line (90°) Input

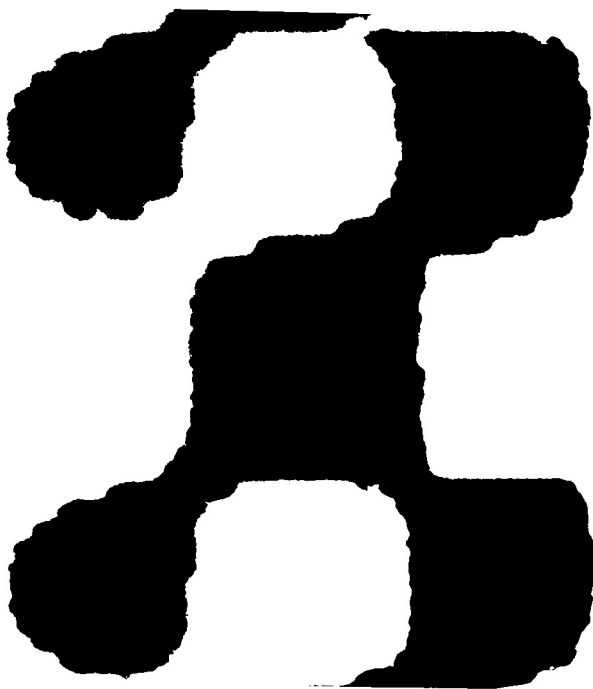


Figure 36. Microphotography: Perpendicular Solid Line (90°) Output

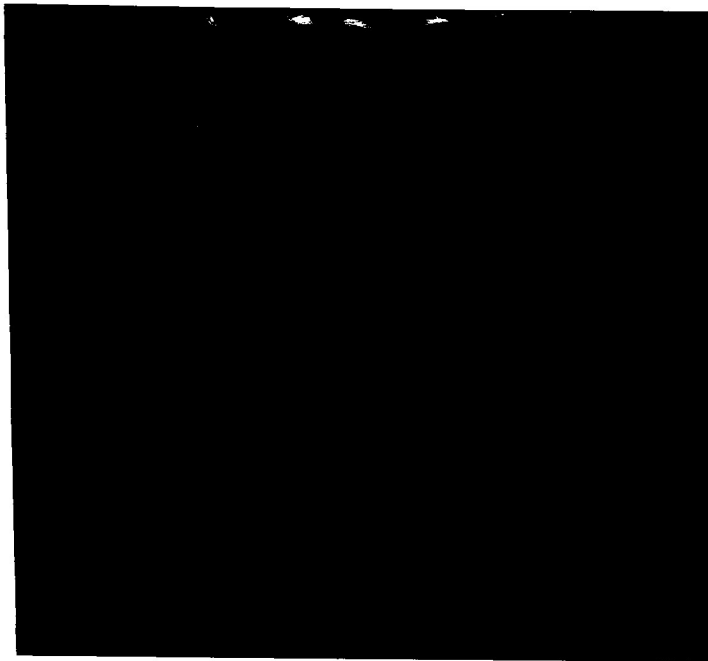


Figure 37. Microphotography: Solid Patch Input

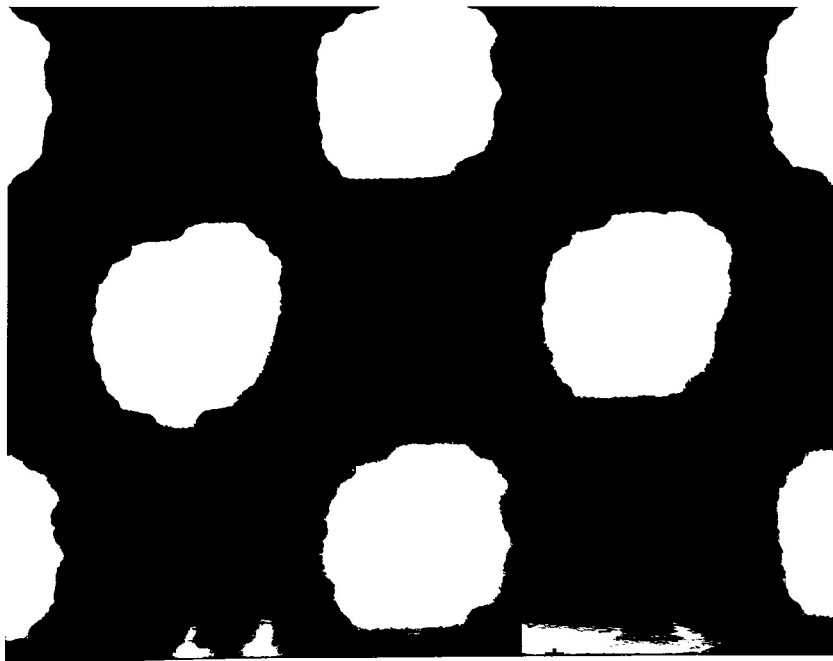


Figure 38. Microphotography: Solid Patch Output

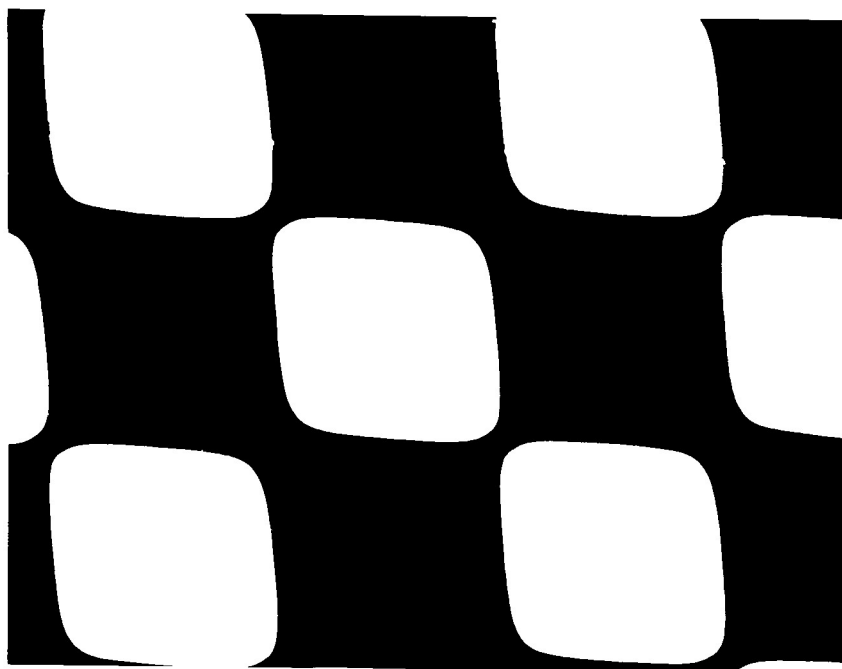


Figure 39. Microphotography: 60% Dot Input

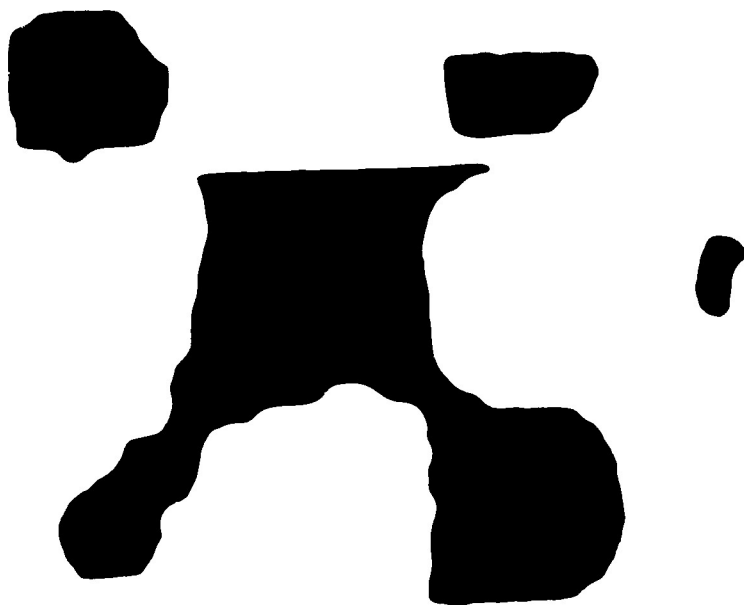


Figure 40. Microphotography: 60% Dot Output

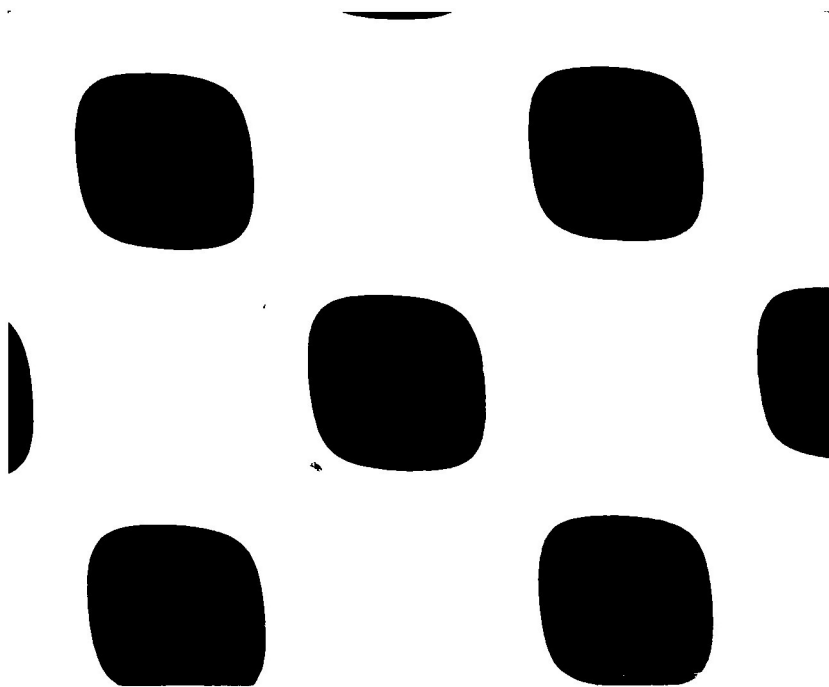


Figure 41. Microphotography: 30% Dot Input

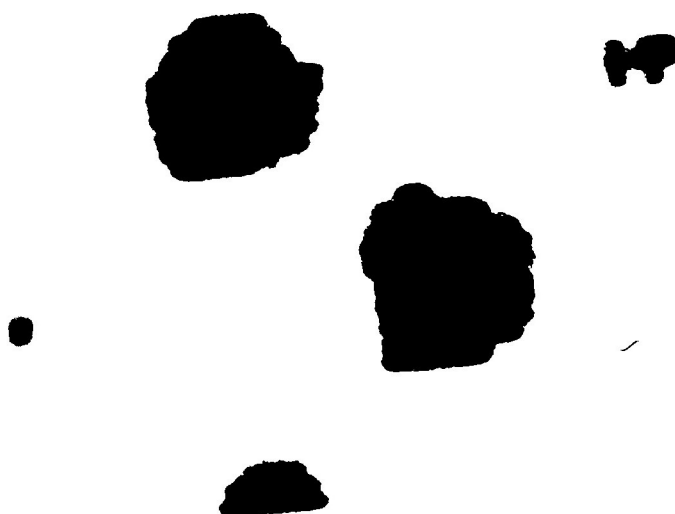


Figure 42. Microphotography: 30% Dot Output

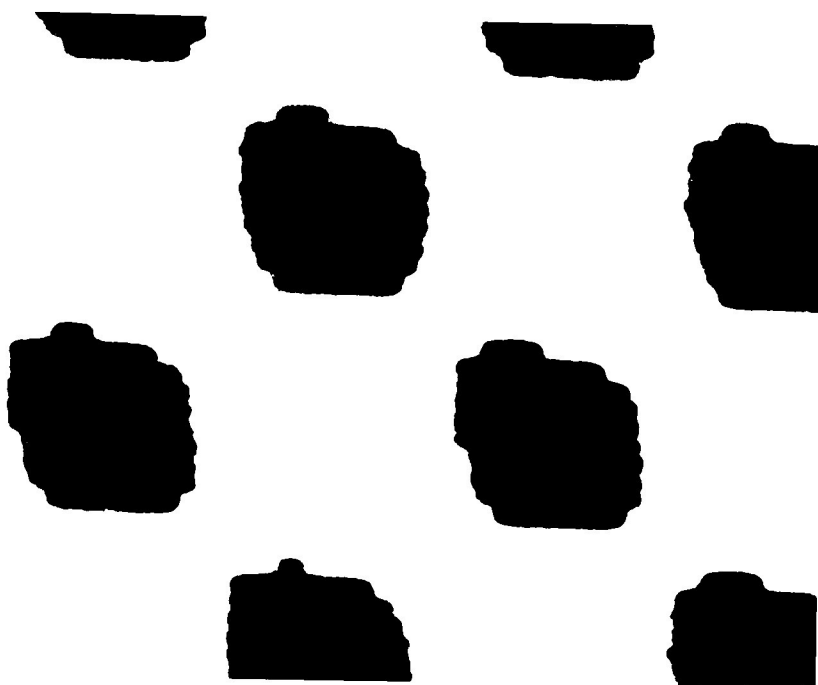


Figure 43. Microphotography: 1.20 Density Output

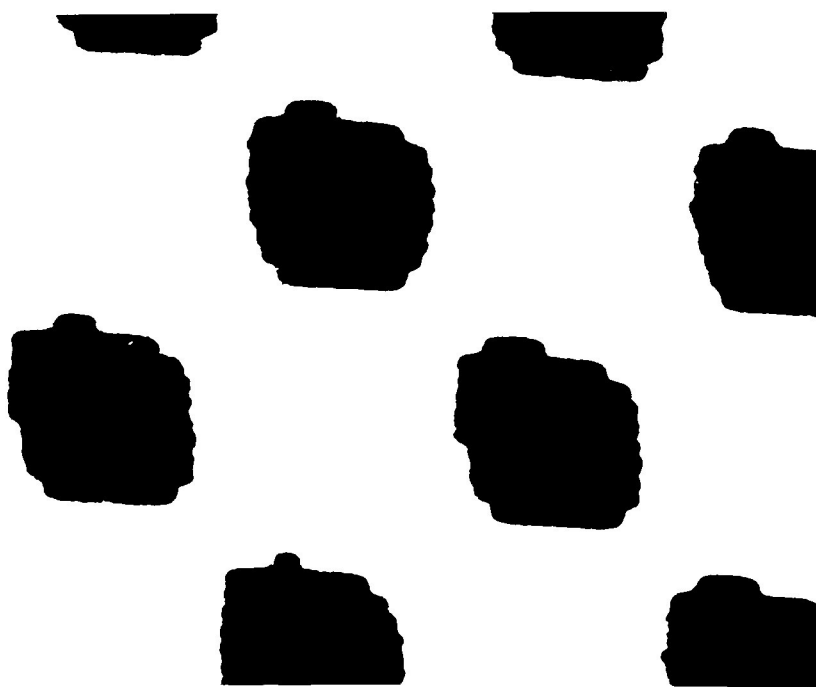


Figure 44. Microphotography: 1.20 Density Output

Chapter VIII

SUMMARY

Conclusions

This paper outlines and details the interworkings of an electronic dot generating scanner. The scanner is a product, which has the flexibility to meet a demanding reproduction process. The printing reproduction process and its many variables require this flexibility to customize the product. The scanner gives the printer the capability to deliver that customized product.

The scanner functions are modeled using optical, electrical, or photography based theories. These theories are applied to the scanning optics, data compression, gradation, color correction, digitization, halftone screening, and film exposure. The scanner is a complex machine because of this integration of different technologies.

The model applies both Fourier and graphical mathematical analysis to represent the scanner functions. Modulation Transfer Functions (MTF's) are calculated to show the frequency characteristics of the scanner optics. Also, the electronic unsharp masking function is modeled optically. A line edge was modeled to show the expected edge enhancement effect. The sharpening of the edge is well shown by the halftone.

The gradation, color correction, halftone screening, enlargement, and film exposure are processes, which the scanner duplicates from the direct screen method of separation. A computer algorithm is created to carry out these functions. These algorithms are more consistent than the human judgement of a camera operator.

The hypothesis states that a mathematical analysis with experimental verification can be developed to accurately model the internal optics, tone reproduction, and output dot

characteristics of an electronic dot generating scanner. The model does have several shortcomings, which made achievement of the hypothesis not possible. These shortcomings are caused by the limited access for detailed electrical analysis, color correction complexities, and lack of detailed component information.

The main accomplishment of this paper was the modeling of the internal optics of the scanner. The MTF's demonstrate the effect of aperture diameter on the resolution of the entire scanner system. The frequency spectrum detected by the system decreases as the aperture diameter increases. A smaller aperture diameter produces better system resolution.

The process of developing this model involved computer science, mathematics, optics, and tone reproduction, which demonstrates again the complexity of the scanner. The study did prove that a model could be developed detailing the basic scanner system from input optics through the final separation.

Recommendations For Future Study

This study should be continued with an examination of the workings of the color computer. The basic study should begin with an understanding of the Neugebauer equations. The challenge will be to account for and model the electrical corrections that are performed for proper color corrections. The scanner applies a modified Neugebauer equation to perform color correction. An examination of this problem would be an excellent project for a future graduate student.

BIBLIOGRAPHY

- Bellis Jr., Donald C. & Moon, James E., "Technical Analysis of Electronic Color Theory, Applications, and Techniques." *Proceedings of the Technical Association of the Graphic Arts*, 1981: 231-250.
- Bevington, Philip R., *Data Reduction and Error Analysis For The Physical Sciences*. New York: McGraw-Hill Book Company, 1969.
- Billmeyer, Jr., Fred W. & Saltzman, Max, *Principles of Color Technology*, 2nd Edition. New York: John Wiley & Sons, Inc., 1981.
- Bruno, Michael H., *Principles of Color Proofing: A Manual on the Measurement and Control of Tone and Color Reproduction*. Salem, New Hampshire: GAMA Communications, 1986.
- Castleman, Kenneth R., *Digital Image Processing*. Englewood Cliffs, New Jersey: Prentice-Hall Inc., 1979.
- DeLorenzo, Joseph D., "Print Quality and Legibility: What are the Ingredients?" *Datek Print Quality Seminar*, Bedford, MA, June 2, 1985.
- DeLorenzo, J.D. & Garsin, P.A., "Image Shaping In Nonlinear Xerographic Systems," *Fourth International Conference on Electrophotography*, Washington, D.C., November 1981.
- Driscoll, Walter G. & Vaughan, William, *Handbook of Optics*. New York: McGraw-Hill Book Company, 1978.
- Eastman Kodak Company, "The Color-Separation Scanner - Q-78." 1981.
- Fitzgerald, A.E., Higginbotham, David E. & Grabel, Arvin, *Basic Electrical Engineering*. New York: McGraw-Hill, 1975.
- Gaskill, Jack D., *Linear Systems, Fourier Transforms, and Optics*. New York: John Wiley & Sons, Inc., 1978.
- Goodman, Joseph W., *Introduction To Fourier Optics*. New York: McGraw-Hill Book Company, 1968.
- Hecht, Eugene & Zajac, Alfred, *Optics*. London: Addison-Wesley, 1979.
- Howe, D.J., Mauer, R.E., & Yule, J.A.C., "An Analysis of The Optics of The Crossline Screen." *Proceedings of the Technical Association of the Graphic Arts*, 1961: 17-30.

- Johnson, Tony, "Designing Scanner Software To Meet Press Requirements." Proceedings of the Technical Association of the Graphic Arts, 1985: 135.
- Korman, N.I., "Accuracy of Color Reproduction with the Digital Computer - Scanner System of Color Separation." Proceedings of the Technical Association of the Graphic Arts, 1972: 156-166.
- Korman, N.I., "Instrumentation of A Digital Computer - Scanner For Color Separation." Proceedings of the Technical Association of the Graphic Arts, 1975: 324-333.
- Linfoot, E.H., Fourier Methods of Optical Image Evaluation. London - New York: Focal Press, 1960.
- Mansfield, Edwin, Statistics For Business And Economics. New York: W.W. Norton & Company, 1980.
- Oittinen, Pirkko & Saarelma, Hannu, "Quality in Digital Printing Reproduction." Proceedings of the Technical Association of the Graphic Arts, 1985: 621--631.
- Roden, Martin S., Digital and Data Communication Systems. Englewood Cliffs, New Jersey: Prentice-Hall, Inc., 1982.
- Schwartz, Mischa, Information Transmission, Modulation, And Noise, 3rd Edition. New York: McGraw-Hill Book Company, 1980.
- Souders, Matt, The Engineer's Companion. New York: John Wiley & Sons, Inc., 1966.
- Southworth, Miles, Color Separation Techniques. Livonia, New York: Graphic Arts Publishing, 1979.
- Welford, W.T., Optics. New York: Oxford University Press, 1981.
- Williams, Charles S. & Becklund, Orville A., Optics - A Short Course for Engineers and Scientists. New York: John Wiley & Sons, Inc., 1972.
- Zhang, Qungpu, "Applications of Colour Scanners in the Reproduction of Remote Sensing Images." Proceedings of the Technical Association of the Graphic Arts, 1983: 668-688.

APPENDIX A

Glossary of Terms

Autocorrelation Theorem -

If $\mathcal{F}\{g(x,y)\} = G(f_x, f_y)$, then

$$\mathcal{F}\left\{\int_{-\infty}^{\infty} \int_{-\infty}^{\infty} g(\xi, \eta) g^*(\xi-x, \eta-y) d\xi d\eta\right\} = |G(f_x, f_y)|^2$$

Bandwidth - the frequency spectrum available to transmit a given amount of information.

Bessel Function - a differential equation used in applied mathematics to describe oscillatory motion.

Condenser - An optical element used to concentrate light on a small area.

Convolution Theorem - the convolution of two functions is equivalent to the operation of multiplying the transforms.

If $\mathcal{F}_2\{g(x,y)\} = G(f_x, f_y)$ and $\mathcal{F}_2\{h(x,y)\} = H(f_x, f_y)$, then

$$\mathcal{F}\left\{\int_{-\infty}^{\infty} \int_{-\infty}^{\infty} g(\xi, \eta) h^*(x-\xi, y-\eta) d\xi d\eta\right\} = G(f_x, f_y) H(f_x, f_y)$$

Cutoff Frequency - the point at which no higher frequencies exist in a system.

Demodulation - the process where a wave resulting from modulation is operated on so that a wave results having the same characteristics as the original modulating wave.

Digitization - the process of converting an analog (continuous) electrical signal to a digital (on-off) signal.

END Values - equivalent neutral density is where three overlapping dots produce a neutral gray.

Fourier Transform -

$$\mathcal{F}\{g(x,y)\} = \int_{-\infty}^{\infty} \int_{-\infty}^{\infty} g(x,y) e^{-j2\pi(f_x x + f_y y)} dx dy$$

Gray Component Replacement (GCR) - the third color in a three color overlap is replaced by black in all areas of a separation.

Laser - An acronym for light amplification by stimulated emission of radiation. A device that converts incident electromagnetic radiation of mixed frequencies to discrete frequencies of highly amplified and coherent visible radiation.

Linear System - (a) $f(y,z) = ag(Y,Z)$

$$af_1(y,z) + bf_2(y,z) = ag_1(Y,Z) + bg_2(Y,Z)$$

a,b = constants

y,x = variables

f,g = mathematical functions

Inverse Fourier Transform -

$$\mathcal{F}^{-1}\{G(f_x, f_y)\} = \int_{-\infty}^{\infty} \int_{-\infty}^{\infty} G(f_x, f_y) e^{+j2\pi(f_x x + f_y y)} df_x df_y$$

Modulation - a wave amplitude is varied as a function of the instantaneous value of another wave.

Modulation Transfer Function (MTF) - the absolute value (modulus) of the Optical Transfer Function (OTF).

Optical Transfer Function (OTF) - the normalized transfer function of a system.

Optics - A branch of Physics concentrating on the properties of light and vision. The emphasis is on the generation, propagation and detection of electromagnetic radiation with wavelengths greater than x-rays and shorter than microwaves.

Photomultiplier (PMT) - an electrical device which converts light to electrical voltage.

Quantization - the electronic process of assigning binary levels to a sampled analog signal.

Transfer Function - a model of the effects of a system in the frequency domain.

Under Color Removal (UCR) - a process in which a fixed percentage of cyan, magenta and yellow dot is removed and replaced by an equivalent black dot in the shadows of a separation.

APPENDIX B

Scanner Procedure

The 399ER scanner was set up per the copyrighted instructions of Prof. Miles Southworth. A copy of this procedure can be obtained by contacting Prof. Southworth at Rochester Institute of Technology.

An UGRA wedge and a gray scale were mounted on the scanning drum for the tone reproduction portion of this study. The scanning data was as follows: enlargement - none, screen ruling - 150 lines/inch, and an aperture stop - 7. The scanner repeatability was checked by outputting four transparencies side by side for each scan. The scanner had excellent repeatability. The data in Table 6 is for one scan of the gray scale.

The microphotography transparencies were mounted in this order: gray scale, UGRA wedge, and a reversed gray scale. The scanning data was as follows: enlargement - 300%, screen ruling - 150 lines/inch, and an aperture stop - 4. The output produced was two side by side.

Scanning Data

Input Density	% Dot Output
0.10	9
0.15	13
0.20	16
0.25	22
0.30	26
0.35	30
0.40	34

0.45	37
0.50	39
0.60	45
0.70	52
0.80	57
0.90	62
1.00	66
1.10	70
1.20	72
1.30	76
1.40	79
1.50	81
1.60	84
1.70	86
1.80	88
1.90	89
2.00	91
2.10	92
2.20	93
2.30	94
2.40	95
2.50	95
2.60	96
2.70	97
2.80	98

2.90	98
3.00	99

Table 6. Tone Reproduction Data

APPENDIX C

Microphotography Equipment and Procedures

Equipment:

- 1) Olympus BH-2 Microscope with Tungsten-Halogen Lamp
- 2) Nikon Multiphot Photographic Attachment

Magnification:

Enlargement: 66X

Materials:

Film: Polaroid Type 55 - Positive/Negative Instant Sheet Film

Film Size: 4 x 5 inches

Procedure:

Separation Positive

Exposure Time: 0.5 seconds

Separation Negatives

Sodium Sulfite Bath: to remove backing

Wetting Agent: to improve development

Film Development:

Time: 20 seconds

B/W Prints

Equipment:

- 1) Olympus Enlargement Camera

Magnification:

Enlargement: None

Materials:

Film: Ilfospeed Multigrade II - Glossy, Medium wt.

Film Size: 8 x 10 Inches

Procedure:

Exposure Time: 10 seconds

Film Development:

Type: Tray

Time: Developer - 1 minute

Stop - 15 seconds

Fix - 2 minutes

APPENDIX D

Microcomputer Equipment and Software

Equipment:

Microcomputer: IBM PC-AT with Hercules Graphics Card and 80287 Coprocessor

Accessories: Laser Printer

Software:

Main Program: HFT Plus

Written by: Dr. John Hayes Techware Inc. - Tucson, AZ

Modified by: Dr. Roger L. Easton - Rochester Institute of Technology

Software Listing:

This software for calculating the basic Fourier transforms and their multiplication and subtraction was applied on this project per the mathematical equations discussed in Chapter VI.

Basic Fourier Transform Calculation

Comments: The 2d FFT, IFT, or incoherent MTF can be computed by this software. It reads a 64 x 64 data array stored with a BLOAD option (8087 or MSoft format). The array fills the center of a 100 x 100 integer array usable by a DPLOT routine or as a 64 x 64 integer halftone array printed by a LIGHTWRITER laser printer. It requires a "87BASRUN.EXE" operating system.

```
OPTION BASE 1
DEFINT I-N
DIM FREAL (64,64), FIMAG(64,64), ARRAY%(100,101)
PI = 3.141593
```

```
ON ERROR GOTO 500
```

```

LN=6
FLN=LN
N=2^LN
QUIT$=""
DRV$="C"
IFMAT=O:FMT$="8087"
FN$="TEST"
FR$="TEST-R":FI$="TEST-I"

```

MAIN PROGRAM:

```

WHILE QUIT$ <> "Y" AND QUIT$ <> "y"
    V$=""
    WHILE V$ <> CHR$(27) AND V$ <> CHR$(13) AND V$ <> "Q"
        GOSUB 1000
    WEND
    PRINT "Quit ... Are you sure (Y/N)?"
    QUIT$=INPUT$(1)
WEND
CLS
END

```

500 ERROR TRAP

```

    WHILE ERR=53
        PRINT "ERROR: File Not Found."
        RESUME 1000
    WEND

    PRINT "Error Number : "ERR
    PRINT "Aborting."
    END

```

BEGIN SUBROUTINES

```

1000 READ MENU
    GOSUB 1200 'print menu
    V$=INPUT$(1)
    IF ASC(V$)>90 THEN V$=CHR$(ASC(V$)-32) 'convert to upper case
    WHILE V$="D"
        D$=DRV$
        INPUT "Drive letter = ":DRV$
        IF DRV$=CHR$(27) OR DRV$=CHR$(13) THEN DRV$=D$
        DRV$=LEFT$(DRV$,1)
    WEND
    V$=""
    WEND

```

'Read Files

```

        WHILE V$="R"
            GOSUB 1300      'read filename
            GOSUB 1200
            GOSUB 1400      'read files
            V$=""
        WEND

'Save Files for DPlot Display
        WHILE V$="S"
            GOSUB 1300      'read filename
            GOSUB 1200
            GOSUB 1600      'save files
            V$=""
        BEEP
        WEND

'BSAVE Files
        WHILE V$="B"
            GOSUB 1300      'read filename
            GOSUB 1200
            GOSUB 1670      'BSAVE 64 x 64 file
            V$=""
        WEND

'Save Halftone Files
        WHILE V$="H"
            GOSUB 1300      'read filename
            GOSUB 1200
            GOSUB 1650      'save files
            V$=""
        BEEP
        WEND

'Take FFT
        WHILE V$="F"
            PRINT "Checkerboard phase shift";
            GOSUB 2100      'phase shift
            PRINT "Taking FFT ...";
            CALL FFT2D(FREAL(1,1),FIMAG(1,1), FLN)
            PRINT "Finished."
            PRINT "Checkerboard phase shift";
            GOSUB 2100      'phase shift
            BEEP
            V$=""
        WEND

'Take Inverse FFT
        WHILE V$="I"
            PRINT "Checkerboard phase shift";
            GOSUB 2100      'phase shift

```

```

    PRINT "Taking IFT ...";
    CALL IFT2D(FREAL(1,1), FIMAG(1,1), FLN)
    PRINT "Finished."
    PRINT "Checkerboard phase shift";
    GOSUB 2100                                'phase shift
    BEEP
    V$=""
    WEND

```

```

'Take Squared Magnitude
    WHILE V$="M"
        PRINT "Squared-Magnitude"
    GOSUB 2200
    V$=""
    WEND

```

```

"Take Complex Reciprocal
    WHILE V$="D"
        PRINT "Complex Reciprocal"
    GOSUB 2300
    V$=""
    WEND

```

```

    WHILE V$="L"
        INPUT "Enter name of output line file";FA$
        FAE$ = DRV$ + ":" + FA$ + ".DAT"
        OPEN FAE$ FOR OUTPUT AS #1
            INPUT "store which line of data (1-64)"; L1
            FOR J = 1 TO 64
                WRITE #1, FREAL(L1,J)
            NEXT J
        CLOSE #1
    WEND

```

```

    BEEP
    V$=""
    WEND

```

```

    RETURN

```

1200 PRINT DEFAULT MENU

```

LOCATE 1,1
PRINT "UNSHARP Command Menu (ver 1.2)"
PRINT STRING$(12,205)
PRINT "[D] Default DRIVE.....";DRV$
PRINT "[R] READ data (64 x 64) .....";("FR$",";FI$")
PRINT "[S] SAVE data (100 x 100) ....";("FR$",";FI$")
PRINT "[H] save HALFTONE data (64 x 64)
PRINT "[B] BASVE array (64 x 64) for other operation"
PRINT
PRINT "[F] Take FFT"
PRINT "[I] Take IFT"

```

```

PRINT "[M] Squared MAGNITUDE
PRINT "[D] Complex Reciprocal {1/[array]}
PRINT "[L] Store LINE of Data"
PRINT "[Q] QUIT "
PRINT
PRINT "Command:?",SPACE$(60)
PRINT SPACE$(240);
PRINT SPACE$(240);
LOCATE CSRLIN-6,1
RETURN

```

1300 READ FILENAME

```

FSAV$=FN$
INPUT "Filename (four characters) = "; FN$
IF FN$=CHR$(27) THEN RETURN ELSE IF FN$=CHR$(13) THEN
  FN$=FSAV$
FR$=DRV$+"."+LEFT$(FN$,6)+"-R.DAT"
FI$=DRV$+"."+LEFT$(FN$,6)+"-I.DAT"
RETURN

```

1400 READ DATA (64 x 64)

```

F$=FI$
GOSUB 1500          'load image from disk into real array
GOSUB 3800          'load image array with real array
F$=FR$
GOSUB 1500          'load real array from disk
IF IFMAT=1 THEN GOSUB 5000 'convert to IEEE if MSoft
RETURN

```

1500 READ DATA FROM DISKFILE -- USING BLOAD OPTION

```

PRINT "Reading File: ";FILES F$
BLOAD F$, VARPTR(FREAL(1,1))
RETURN

```

1600 WRITE REAL & IMAG FILES (100 x 100) TO DISK

```

GOSUB 3000          'find qnorm for freal
GOSUB 4000          'transfer to ARRAY%
F$=FR$
GOSUB 1700          'save data to disk
GOSUB 3700          'transfer fimag to freal
GOSUB 3000          'find qnorm for freal
GOSUB 4000          'transfer to ARRAY%
F$=FI$
GOSUB 1700          'save data to disk
RETURN

```

1650 WRITE HALFTONE FILES (64 x 64) TO DISK


```

GOSUB 3100      'scale freal for halftone
  F$=FR$
GOSUB 4100      'write data file from ARRAY% to F$
GOSUB 3700      'transfer fimag to freal
PRINT "FILE TRANSFERRED"
GOSUB 3100      'scale freal for halftone
  F$=FI$
GOSUB 4100      'write data file from ARRAY% to F$
RETURN

```

1670'WRITE 64 x 64 FILES FOR FURTHER USE

```

  F$=FR$
  PRINT "SAVING FILE ",F$
  BSAVE F$,VARPTR(FREAL(1,1),16384
GOSUB 3700
  F$=FI$
  PRINT "SAVING FILE ",F$
  BSAVE F$,VARPTR(FREAL(1,1)),16384
RETURN

```

1700'WRITE RANDOM DATA FILE

```

  PRINT "Writing Data File: "F$
  QNORM$=MK$$(QNORM)
  FOR J = 0 TO 1
    ARRAY%(J + 1,101)=CVI(MID$(QNORM$,J*2 + 1,2))
  NEXT
  BSAVE F$,VARPTR(ARRAY%(1,1)),20200
RETURN

```

2100'PHASE SHIFT

```

  FOR I = 1 TO N
  PRINT " ";
    FOR J = 1 TO N
      FREAL(J,I) = FREAL(J,I)*(-1)^((I-1)+(J-1))
      FIMAG(J,I) = FIMAG(J,I)*(-1)^((I-1)+(J-1))
    NEXT
  NEXT
  PRINT
RETURN

```

2200'SQUARED MAGNITUDE

```

  FOR J = 1 TO N
  PRINT " ";
    FOR I = 1 TO N
      W! = FREAL(I,J)^2 + FIMAG(I,J)^2
    NEXT
  NEXT

```

```

        FREAL(I,J) = W!
        FIMAG(I,J) = 0.
    NEXT I: NEXT J
    BEEP
    RETURN

```

2300'COMPLEX RECIPROCAL with apodization

```

    FOR J = 1 TO N
        PRINT " ";
        FOR I = 1 TO N
            W! = FREAL(I,J)^2 + FIMAG(I,J)^2
            IF W! > 0 THEN GOTO 2301
            FREAL(I,J) = 0.
            FIMAG(I,J) = 0.
            GOTO 2302
2301        FREAL(I,J) = FREAL(I,J)/W!
            FIMAG(I,J) = -FIMAG(I,J)/W!
2302    NEXT I: NEXT J
    BEEP
    RETURN

```

3000'FIND MAX, MIN, NORM

```

    YMAX = FREAL(1,1):YMIN = FREAL(1,1)
    FOR I = 1 TO N
        FOR J = 1 TO N
            IF FREAL(J,I) > YMAX THEN YMAX = FREAL(J,I)
            IF FREAL(J,I) < YMIN THEN YMIN = FREAL(J,I)
        NEXT J
    NEXT I
    IF ABS(YMAX) > ABS(YMIN) THEN QNORM = ABS(YMAX) ELSE
    QNORM = ABS(YMIN)
    IF QNORM = 0 THE QNORM = 1
    RETURN

```

3100'FIND MAX, MIN, NORM FOR HALFTONE

```

    YMAX = FREAL(1,1): YMIN = FREAL(1,1)
    FOR I = 1 TO 64
        FOR J = 1 TO 64
            IF FREAL(J,I) > YMAX THEN YMAN = FREAL(J,I)
            IF FREAL(J,I) < YMIN THEN YMIN = FREAL(J,I)
        NEXT J
    NEXT I
    RANGE = YMAX - YMIN
    RETURN

```

3700'FILL FREAL WITH FIMAG

```

FOR I = 1 TO N
  FOR J = 1 TO N
    FREAL(J,I) = FIMAG(J,I)
  NEXT J
NEXT I
RETURN

```

3800'FILL FIMAG WITH FREAL

```

FOR I = 1 TO N
  FOR J = 1 TO N
    FIMAG(J,I) = FREAL(J,I)
  NEXT J
NEXT I
RETURN

```

4000'FILL 100 x 100 ARRAY

```

PRINT "Filling array";
FOR J = 1 TO 64
  FOR I = 1 TO 64
    ELEM = INT(256/QNORM*FREAL(I,J))
    ARRAY%(I+18,J+18) = ELEM
  NEXT I
NEXT J
PRINT
RETURN

```

4100'WRITE 64 x 64 DATA FILE FOR HALFTONE-TONE

```

PRINT "Filling array";
FOR I = 1 TO 64
  FOR J = 1 TO 64
    FREAL(J,I) = 25. * ((FREAL(J,I) - YMIN)/RANGE)
    ARRAY%(J,I) = 57 - INT(FREAL(J,I))
  NEXT J
NEXT I
PRINT
PRINT "Writing Data File: "F$
OPEN F$ FOR OUTPUT AS #1
PRINT #1, 64;
PRINT #1, 64;
FOR J = 1 TO 64
  FOR I = 1 TO 64
    PRINT #1, CHR$(ARRAY%(J,I));
  NEXT I
PRINT #1, CHR$(13);
PRINT #1, CHR$(10);

```

```

      NEXT
    CLOSE #1
  RETURN

```

5000'CONVERT FROM MSOFT TO IEEE FORMAT

```

    INMUM = N*N
    CALL SM2I(FREAL(1,1),FREAL(1,1),INUM)
    CALL SM2I(FIMAG(1,1),FIMAG(1,1),INUM)
  RETURN

```

Multiplication of Two Fourier Transforms

Comments: This program multiplies two 64 x 64 complex arrays point by point,

i.e. $F1 = (a + ib)$, $F2 = (c + id)$, then

$$F1 * F2 = (ac - bd) + i(ad + bc)$$

The files are loaded via BLOAD and saved via BSAVE

```

OPTION BASE 1
DEFINT I-M
DIM FI(64,64), F2(64,64), FOUT(64,64)
PRINT "(a + ib) *(c + id) = (ac - bd) + i(ad + bc)"
INPUT "enter name of first file ",N1$
  NAME1R$ = "C:" + N1$ + ".R.DAT"
  NAME1I$ = "C:" + N1$ + ".I.DAT"

INPUT "enter name of second file ",N2$
  NAME2R$ = "C:" + N2$ + ".R.DAT"
  NAME2I$ = "C:" + N2$ + ".I.DAT"

INPUT "enter name of output file ",NOUT$
  NAME3R$ = "C:" + NOUT$ + ".R.DAT"
  NAME3I$ = "C:" + NOUT$ + ".I.DAT"

'FIND REAL PART OF PRODUCT
'Load and Multiply Real Parts

  BLOAD NAME1R$, VARPTR(F1(1,1))
  BLOAD NAME2R$, VARPTR(F2(1,1))
  PRINT
  PRINT
  PRINT "(ac";

FOR J = 1 TO 64
  FOR I = 1 TO 64
    FOUT(I,J) = FOUT(I,J) - F1(I,J) * F2(I,J)

```

```

    NEXT I
  NEXT J

```

Load and Multiply Imaginary Parts

```

    BLOAD NAME1I$, VARPTR(FF1(1,1))
    BLOAD NAME2I$, VARPTR(F2(1,1))
    PRINT " - bd";

    FOR J = 1 TO 64
      FOUT(I,J) = FFOUT(I,J) - F1(I,J) * F2(I,J)
    NEXT I
  NEXT J

```

'Save Real Part of Product

```

    BSAVE NAME3R$, VARPTR(FOUT(1,1),16384

```

COMPUTE IMAGINARY PART OF PRODUCT

'Load real part of first file, imaginary part of second file

```

    BLOAD NAME1R$, VARPTR(F1(1,1))
    BLOAD NAME2I$, VARPTR(F2(1,1))
    PRINT " + i * (ad";

```

```

    FOR J = 1 TO 64
      FOR I = 1 TO 64
        FOUT(I,J) = F1(I,J) * F2(I,J)
      NEXT I
    NEXT J

```

'Load imaginary part of first file, real part of second file

```

    BLOAD NAME1I$, VARPTR(F1(1,1))
    BLOAD NAME2R$, VARPTR(F2(1,1))
    PRINT " + bc";

    FOR J = 1 TO 64
      FOR I = 1 TO 64
        FOUT(I,J) = FOUT(I,J) + F1(I,J) * F2(I,J)
      NEXT I
    NEXT J

```

"Save imaginary part of product

```

    BSAVE NAME3I$, VARPTR(FOUR(1,1),16384
    PRINT " done"
    BEEP
  END

```

The Subtraction of Two Fourier Transforms

Comments: This program subtracts the incoherent OTF's of the annulus and aperture to simulate the printing scanner operation.
 The signal is normalized to unity at the origin.
 Loads via BLOAD, save via BSAVE
 Given annulus = $a + ib$, aperture = $c + id$,
 computes real part = $2c - a$
 imaginary part = $2d - b$

```
OPTION BASE 1
DEFUBT I -M
DIM F1(64,64), F2(64,64)

INPUT "enter name of aperture file ",NAPER$
NAME1R$ = "C:" + NAPER$ + "-R.DAT"
NAME1I$ = "C:" + NAPER$ + "-I.DAT"

INPUT "enter name of annulus file ",NANNU$
NAME2R$ = "C:" + NANNU$ + "-R.DAT"
NAME2I$ = "C:" + NANNU$ + "-I.DAT"

INPUT "enter name of output file ",NOUT$
NAME3R$ = "C:" + NOUT$ + "-R.DAT"
NAME3I$ = "C:" + NOUT$ + "-I.DAT"

BLOAD NAME1R$ VARPTR(F1(1,1))
BLOAD NAME2R$, VARPTR(F2(1,1))
PRINT "REAL FILES READ"
GOSUB 100
BSAVE NAME3R$, VAARPTR(F1(1,1))
PRINT "REAL FILE SAVED"

BLOAD NAME1I$, VARPTR(F1(1,1))
BLOAD NAME2I$, VARPTR(F2(1,1))
PRINT "IMAGINARY FILES READ"
GOSUB 100
BSAVE NAME3I$, VARPTR(F1(1,1),16384)
BEEP
END
```

'Subroutine to Subtract Arrays

```
100 F1MAX = -1.: F1MIN = +1.: F2MAX = -1.: F2MIN = 1.

FOR J = 1 TO 64
  FOR I = 1 TO 64
    IF F1MAX < F1(I,J) THEN F1MAX = F1(I,J)
    IF F2MAX < F2(I,J) THEN F2MAX = F2(I,J)
    IF F1MIN > F1(I,J) THEN F1MIN = F1(I,J)
```

```

        IF F2MIN > F2(I,J) THEN F2MIN = F2(I,J)
      NEXT I
    NEXT J

```

```

F1RANGE = F1MAX - F1MIN: F2RANGE = F2MAX - F2MIN
PRINT "Maxima are "; F1MAX, F2MAX
PRINT "Minima are "; F1MIN, F2MIN

```

'Scale and subtract arrays

```

FOR J = 1 TO 64
  FOR I = 1 TO 64
    D = (F1(I,J)-F1MIN)/F1RANGE *2.
    E = (F2(I,J)-F2MIN)/F2RANGE
    F1(I,J) = ABS(D-E)
  NEXT I
NEXT J
PRINT "FILES SUBTRACTED"
RETURN
END

```

APPENDIX E

Fourier Optics

Sample Cutoff Range Calculation: $33\mu\text{m} \rightarrow 5 \text{ samples}$

$$33\mu\text{m}/5 \text{ samples} = 6.6\mu\text{m}/\text{sample}$$

in frequency space $1 \text{ cycle}/13.2\mu\text{m} \times 1000 \mu\text{m}/\text{mm} = 76 \text{ cycles}/\text{mm}$

The remaining MTF graphs, halftones, and isometric plots are on the following pages.

These graphs demonstrate the scaling factor, which is the optical spreading difference between the individual lens diameters.

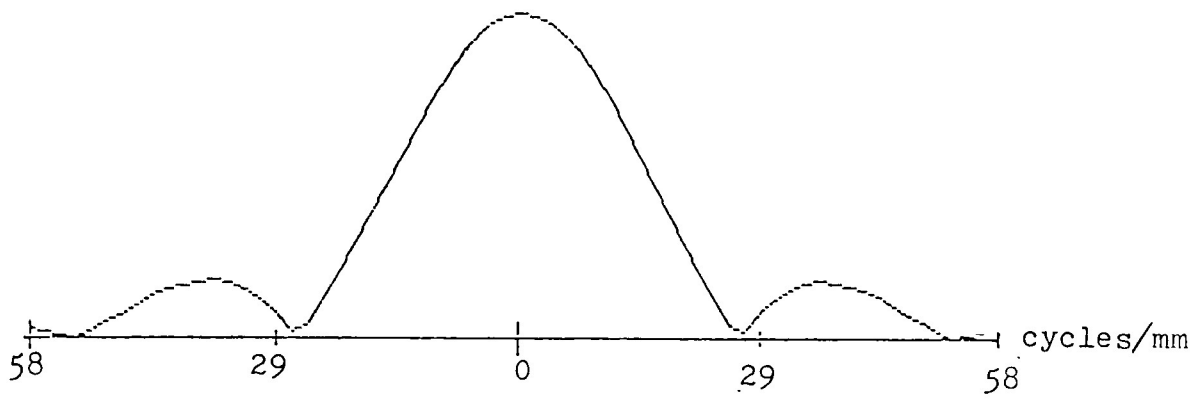


Figure 45. MTF for $a = 43 \mu\text{m}$.

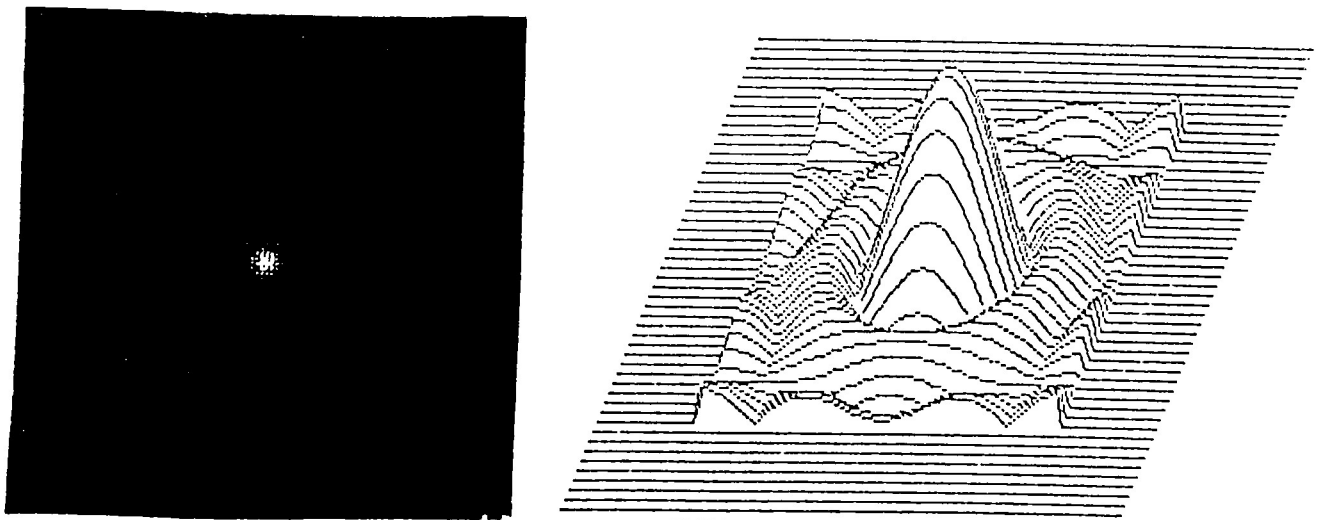


Figure 46. Halftone and Isometric for $a = 43 \mu\text{m}$.

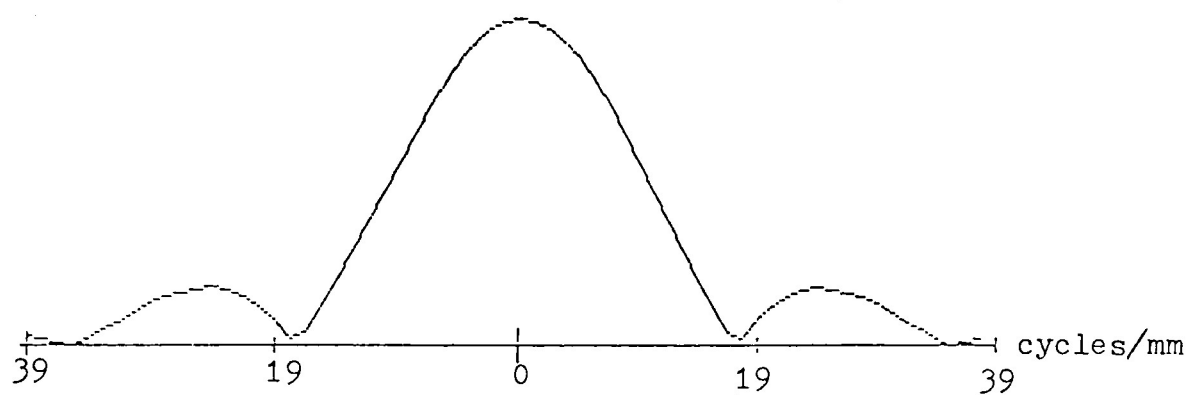


Figure 47. MTF for $a = 64\mu\text{m}$.



Figure 48. Halftone and Isometric for $a = 64\mu\text{m}$.

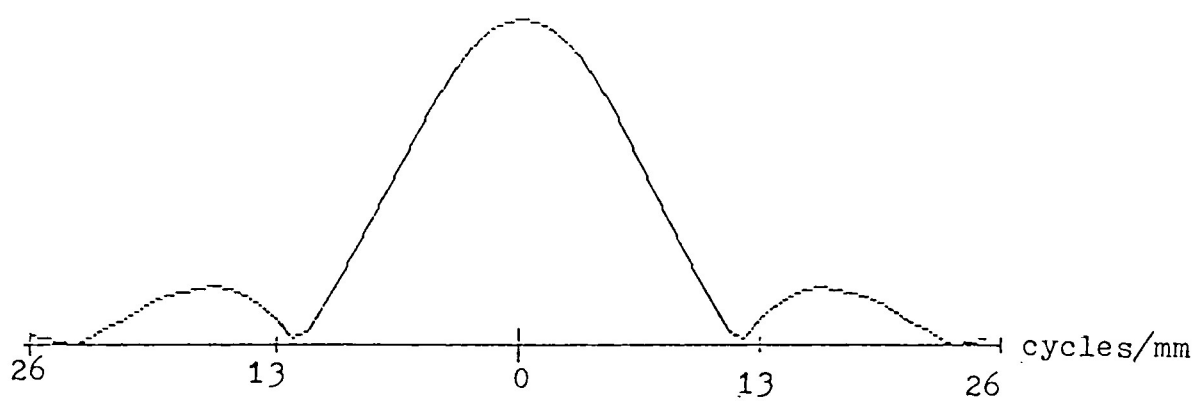


Figure 49. MTF for $a = 96\mu\text{m}$.

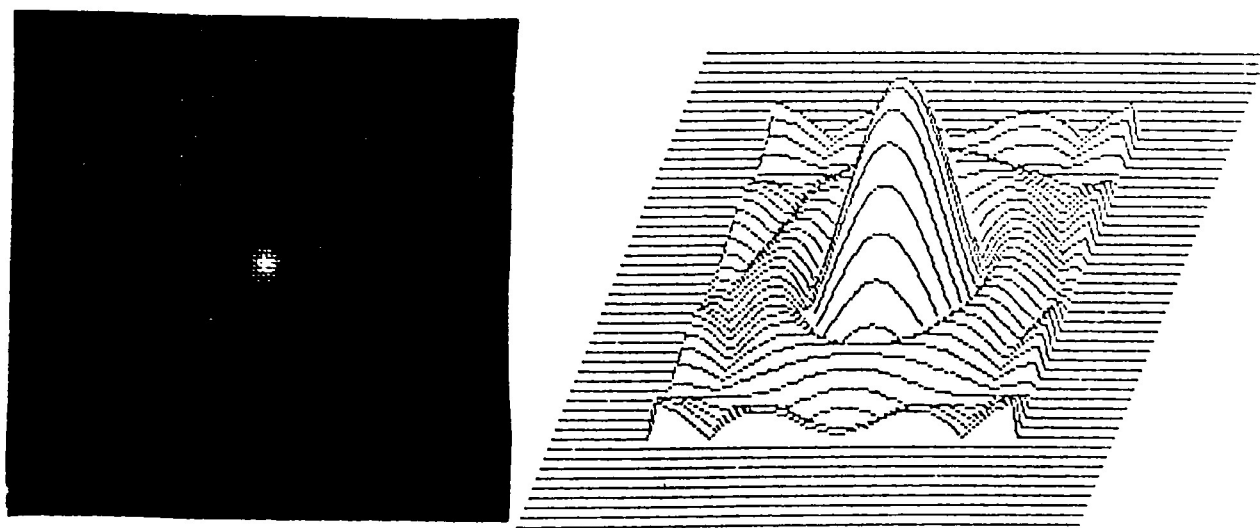


Figure 50. Half-tone and Isometric for $a = 96\mu\text{m}$.

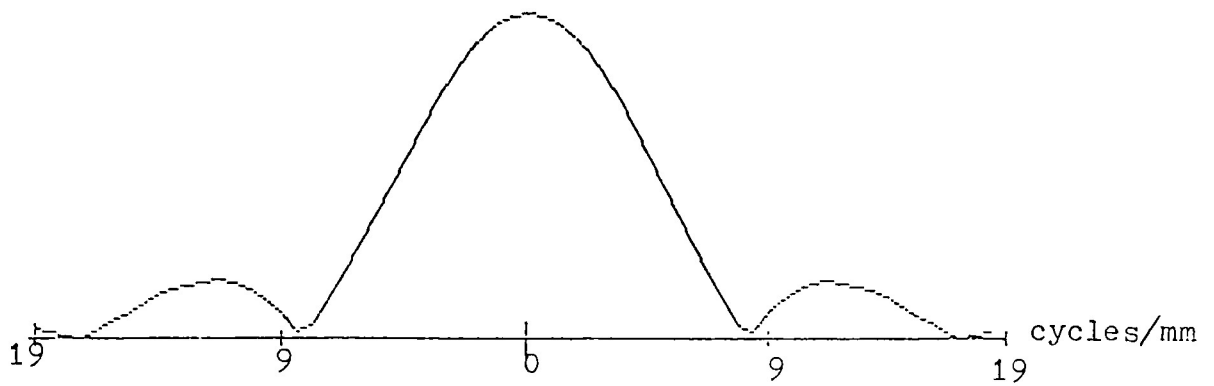


Figure 51. MTF for $a = 130 \mu\text{m}$.

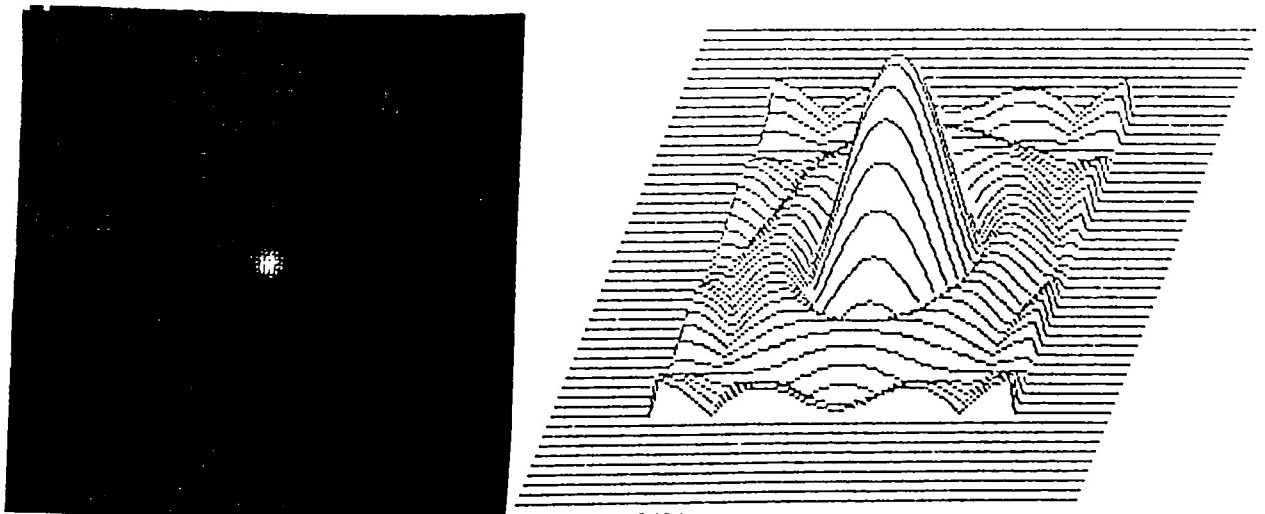


Figure 52. Halftone and Isometric for $a = 130 \mu\text{m}$.

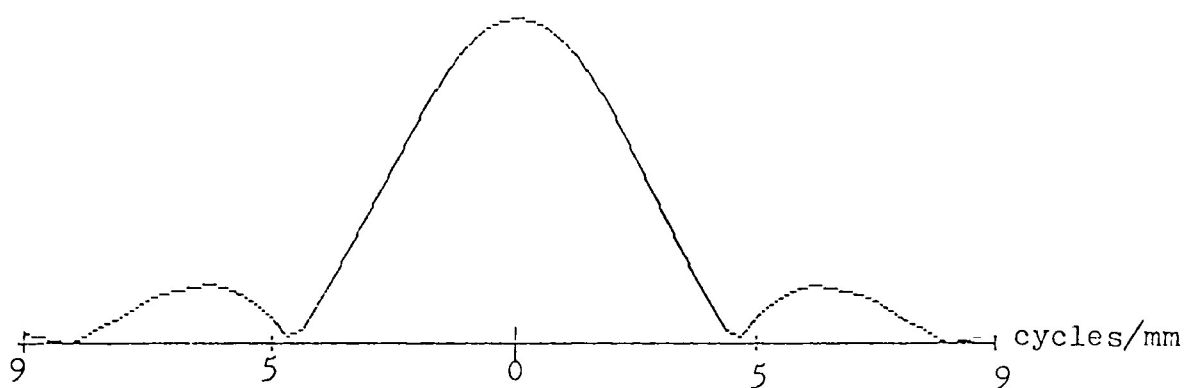


Figure 53. MTF for $a = 270\mu\text{m}$.

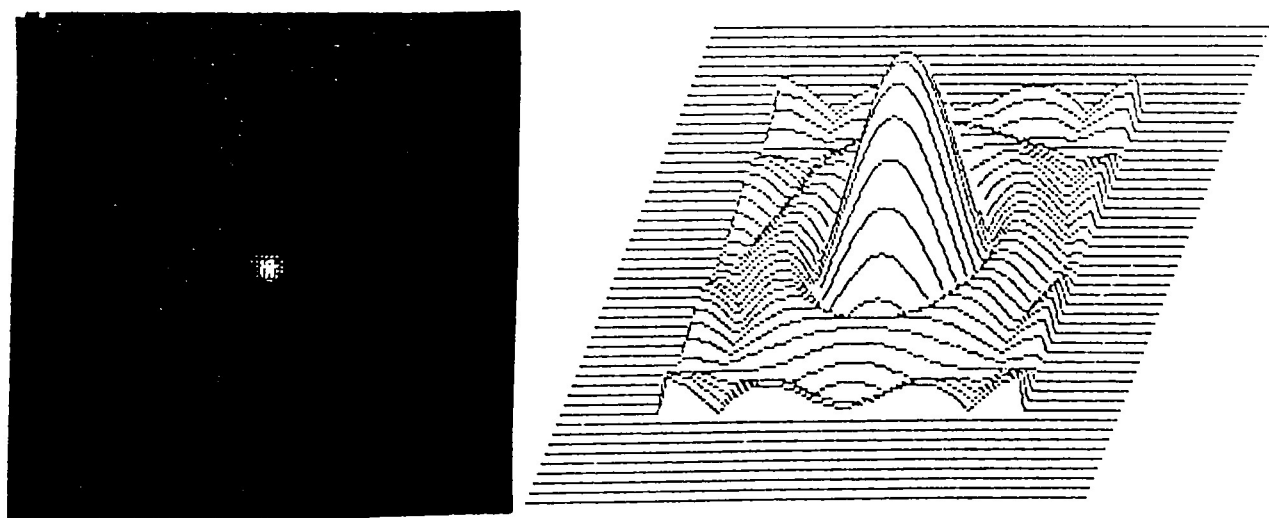


Figure 54. Halftone and Isometric for $a = 270\mu\text{m}$.

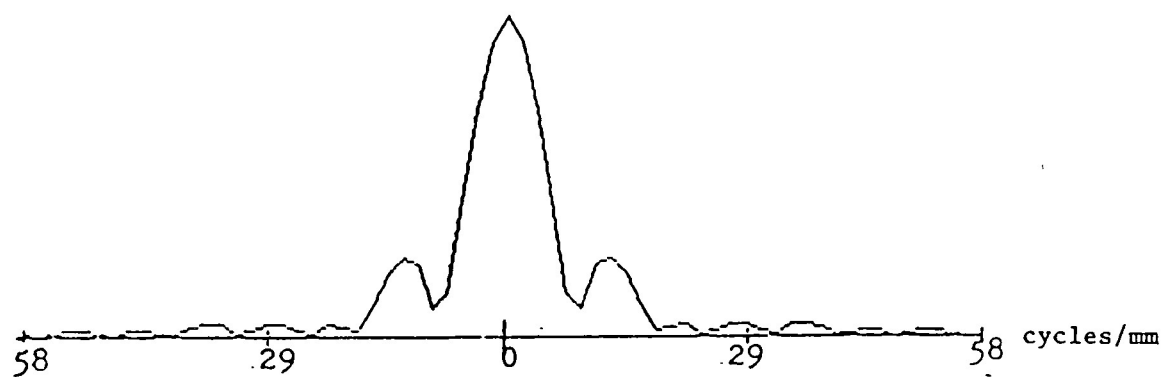


Figure 55. MTF for $a = 43\mu\text{m}$, $b = 126\mu\text{m}$.

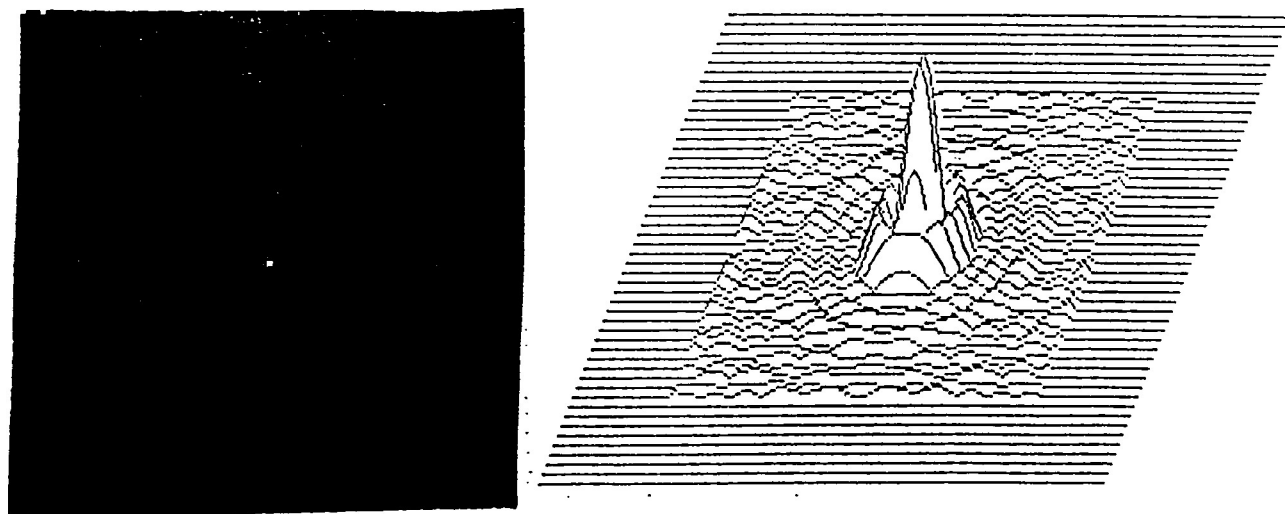


Figure 56. Halftone and Isometric for $a = 43\mu\text{m}$, $b = 126\mu\text{m}$.

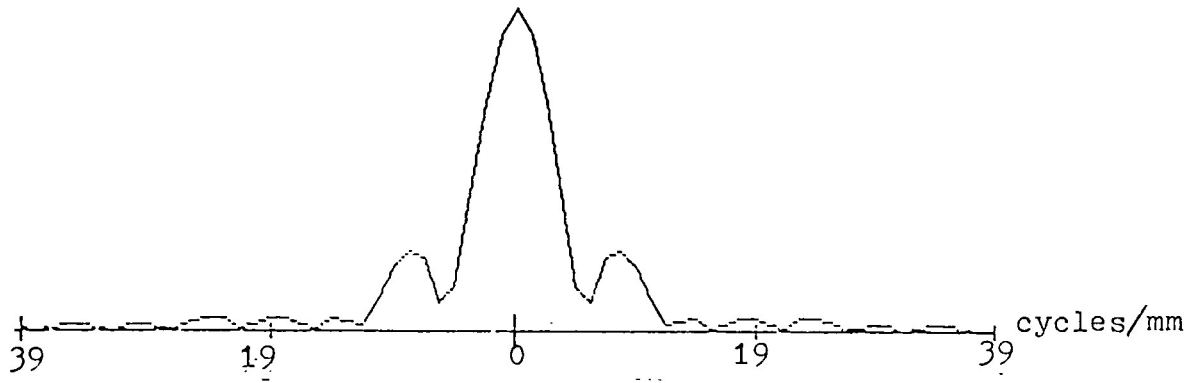


Figure 57. MTF for $a = 64\mu\text{m}$, $b = 192\mu\text{m}$.

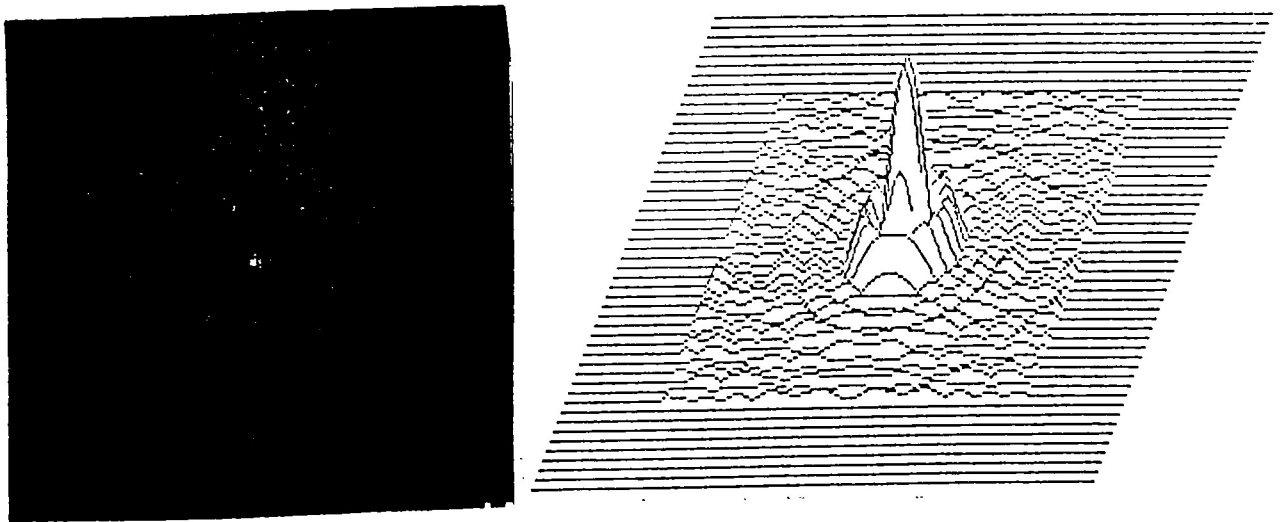


Figure 58. Halftone and Isometric for $a = 64\mu\text{m}$, $b = 192\mu\text{m}$.

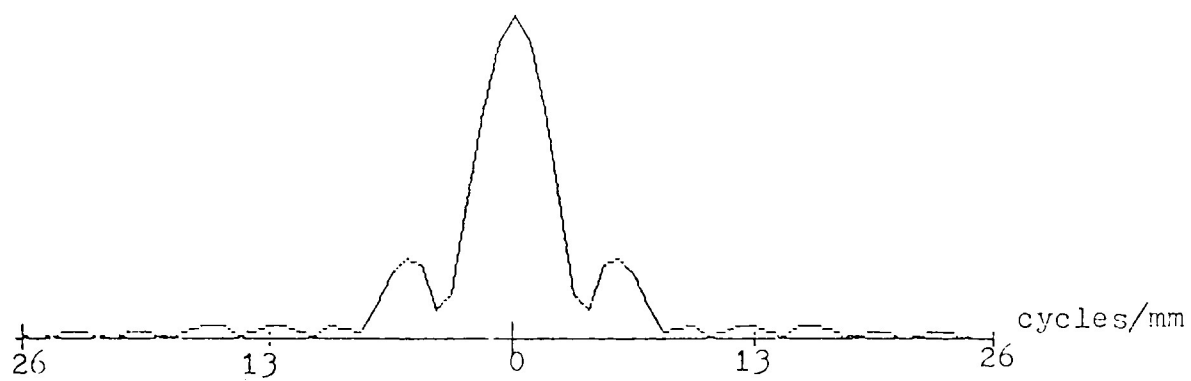


Figure 59. MTF for $a = 96\mu\text{m}$, $b = 288\mu\text{m}$.

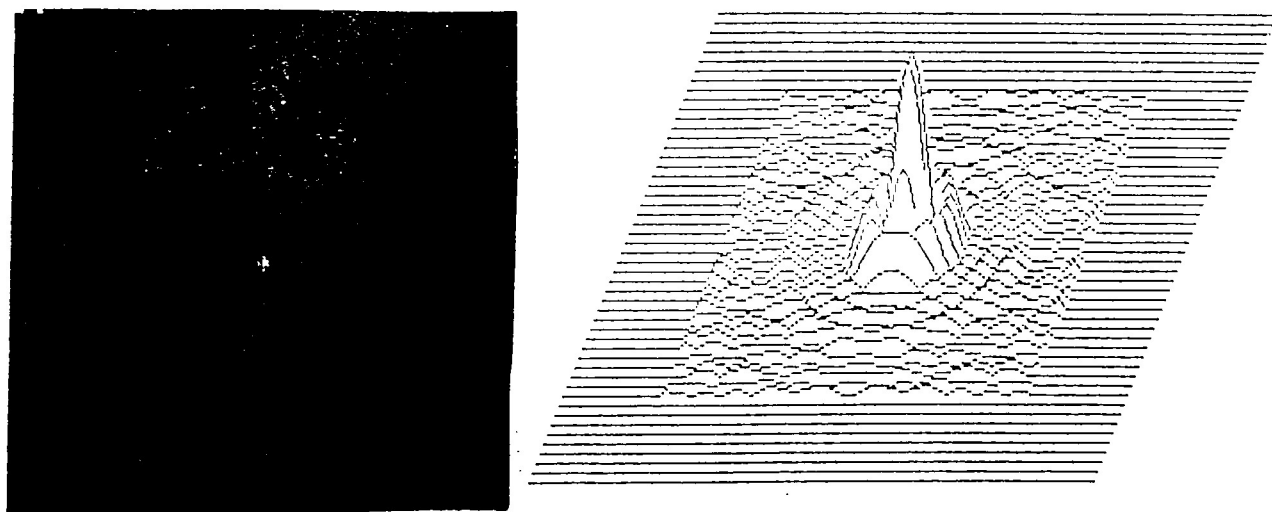


Figure 60. Halftone and Isometric for $a = 96\mu\text{m}$, $b = 288\mu\text{m}$.

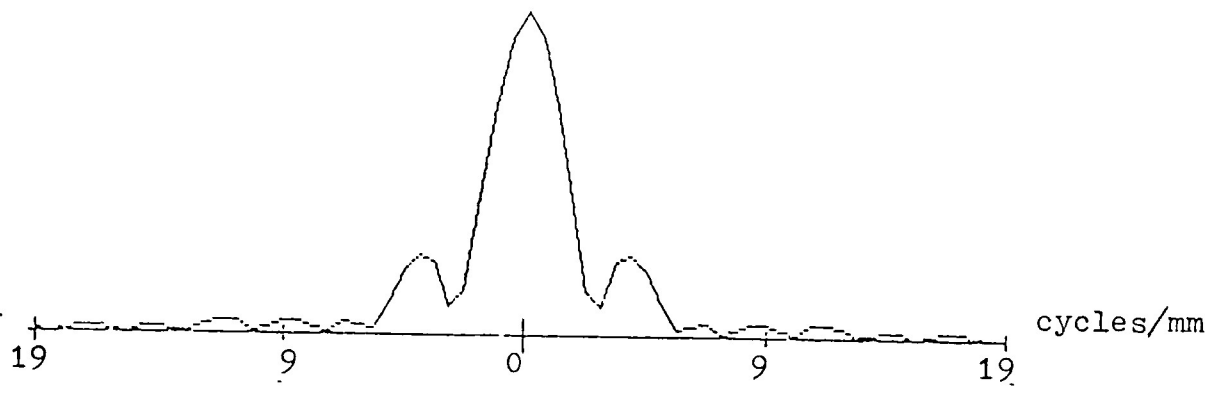


Figure 61. MTF for $a = 130\mu\text{m}$, $b = 390\mu\text{m}$.

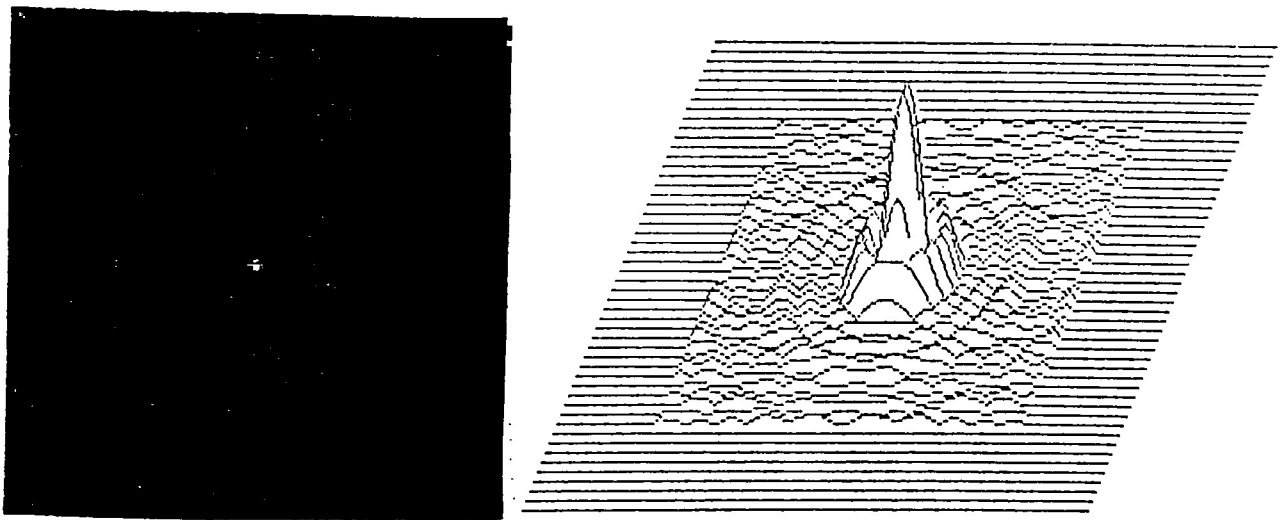


Figure 62. Halftone and Isometric for $a = 130\mu\text{m}$, $b = 390\mu\text{m}$.

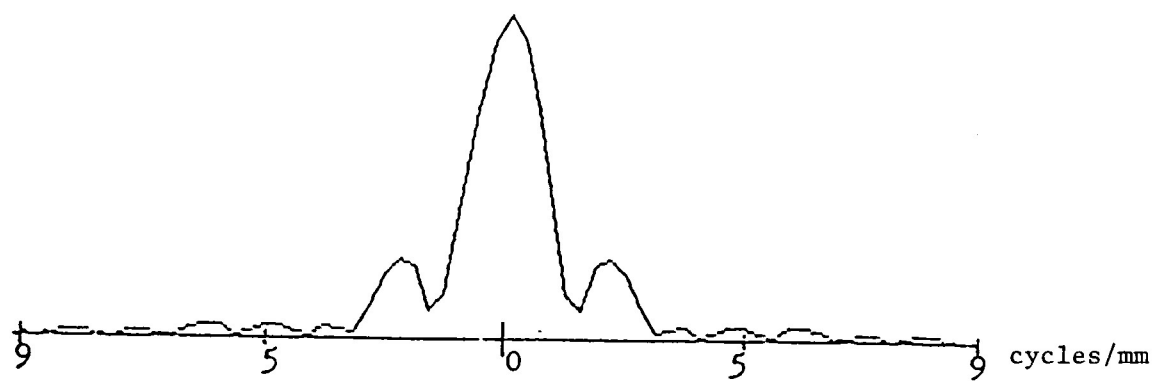


Figure 63. MTF for $a = 270\mu\text{m}$, $b = 810\mu\text{m}$.

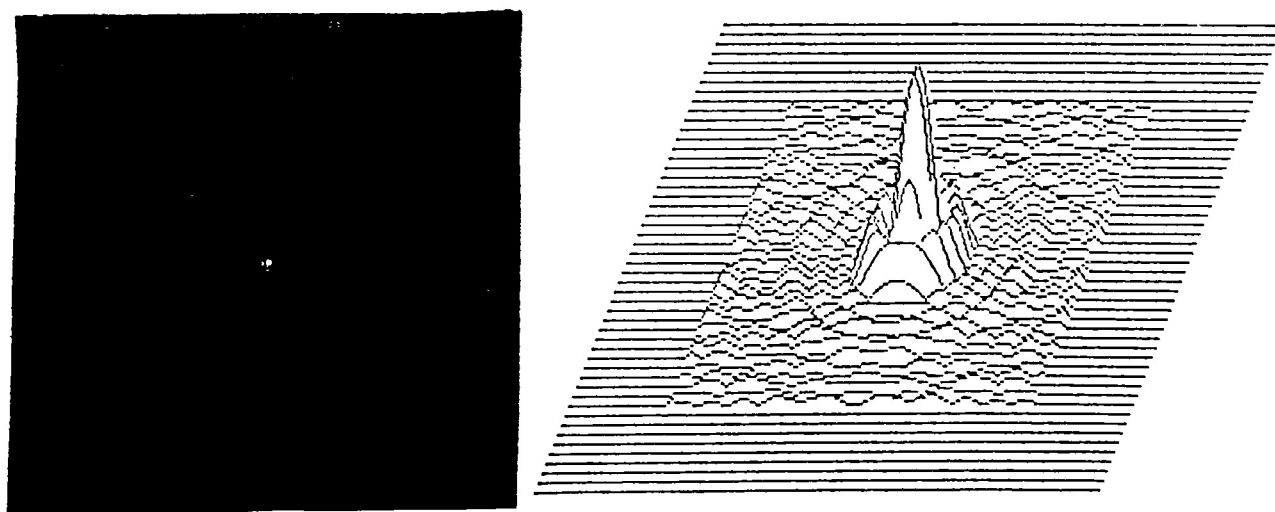


Figure 64. Halftone and Isometric for $a = 270\mu\text{m}$, $b = 810\mu\text{m}$.

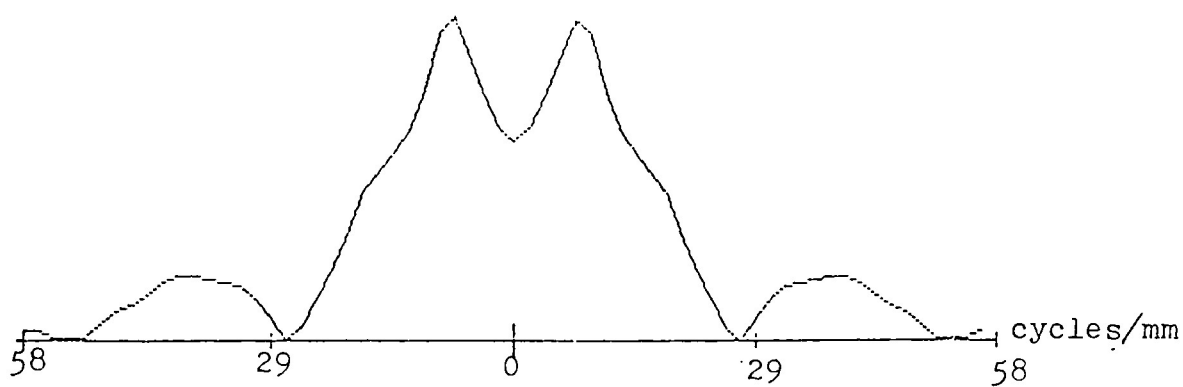


Figure 65. MTF for $a = 43\mu\text{m}$, $b = 126\mu\text{m}$.

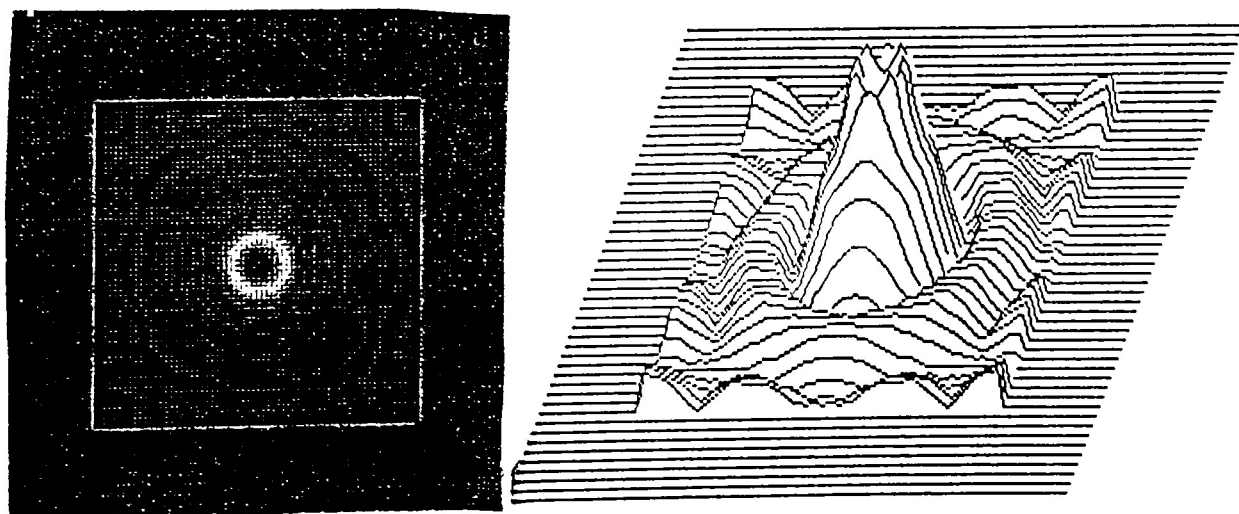


Figure 66. Half-tone and Isometric for $a = 43\mu\text{m}$, $b = 126\mu\text{m}$.

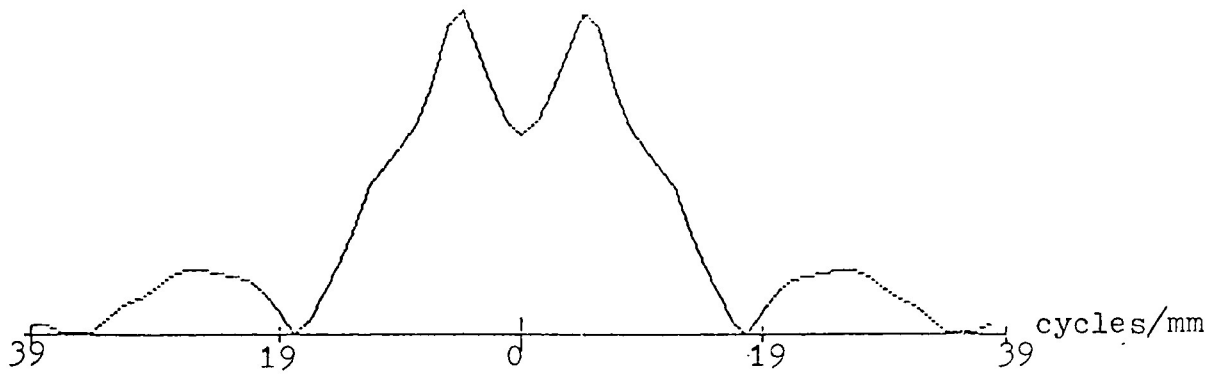


Figure 67. MTF for $a = 64\mu\text{m}$, $b = 192\mu\text{m}$.

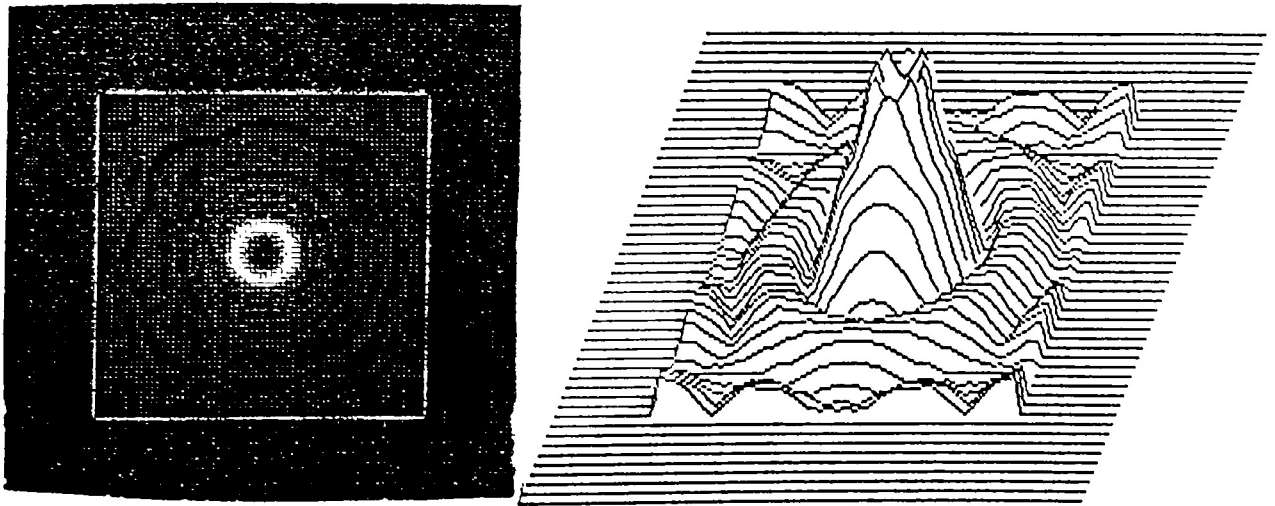


Figure 68. Halftone and Isometric for $a = 64\mu\text{m}$, $b = 192\mu\text{m}$.

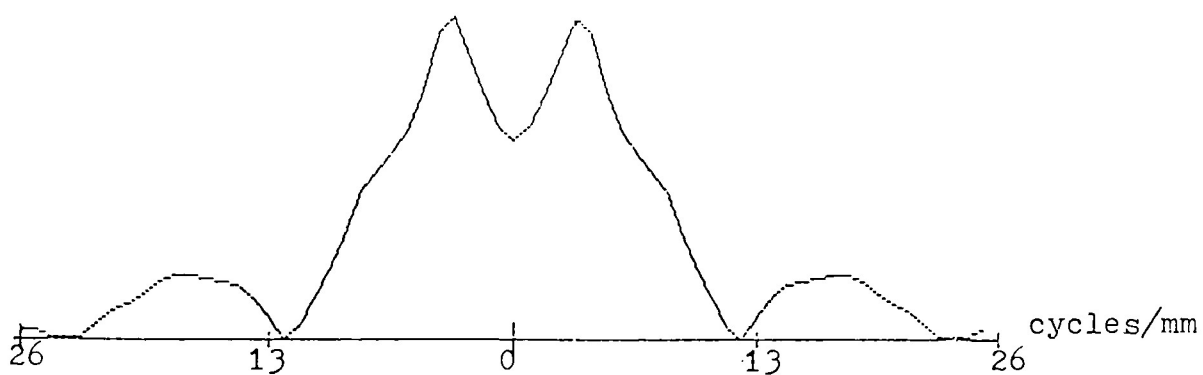


Figure 69. MTF for $a = 96\mu\text{m}$, $b = 288\mu\text{m}$.

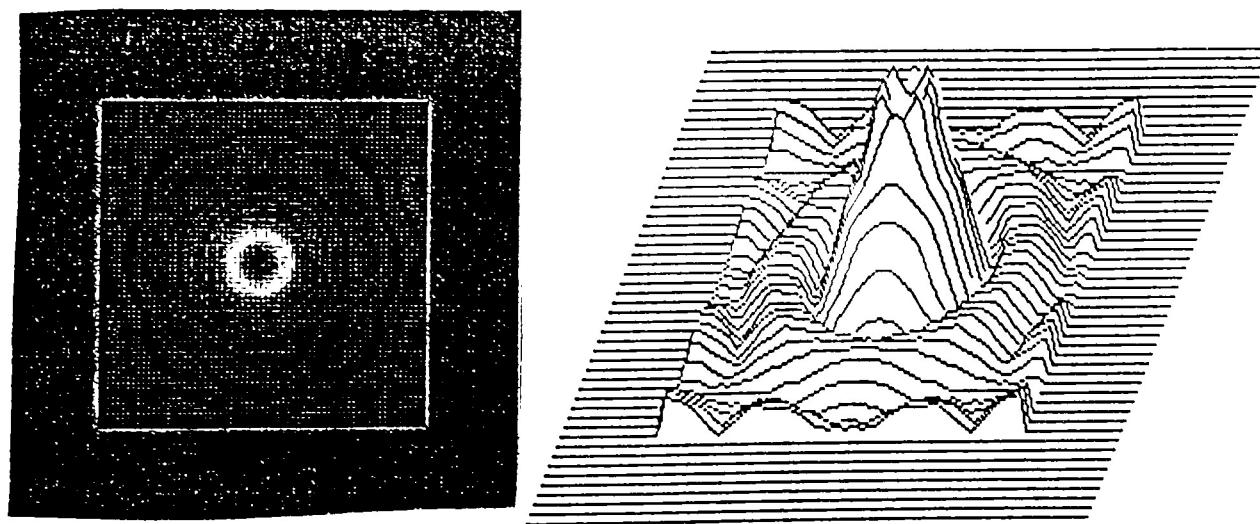


Figure 70. Halftone and Isometric for $a = 96\mu\text{m}$, $b = 288\mu\text{m}$.

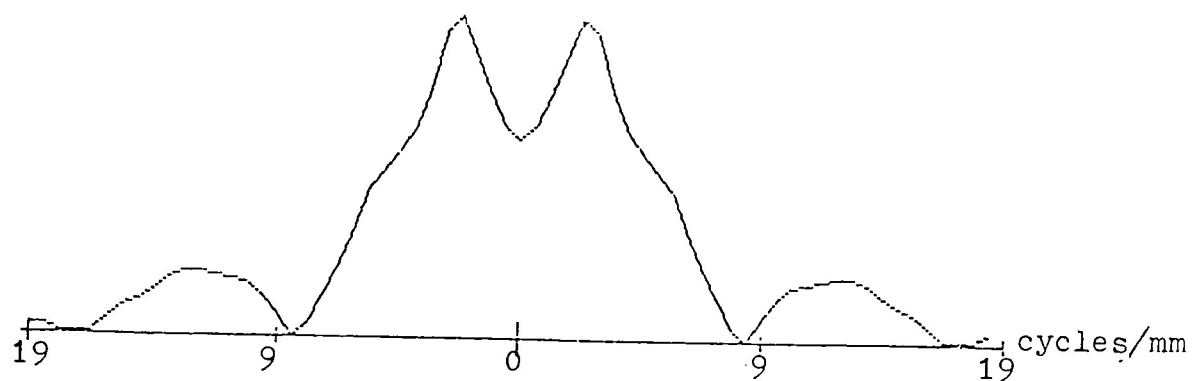


Figure 71. MTF for $a = 130\mu\text{m}$, $b = 390\mu\text{m}$.

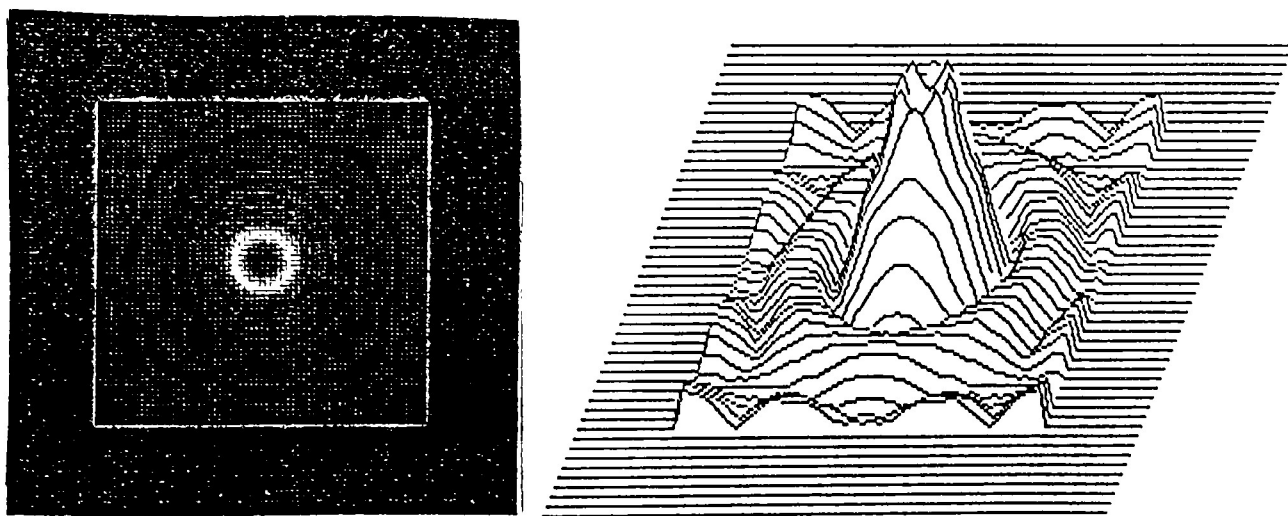


Figure 72. Halftone and Isometric for $a = 130\mu\text{m}$, $b = 390\mu\text{m}$.

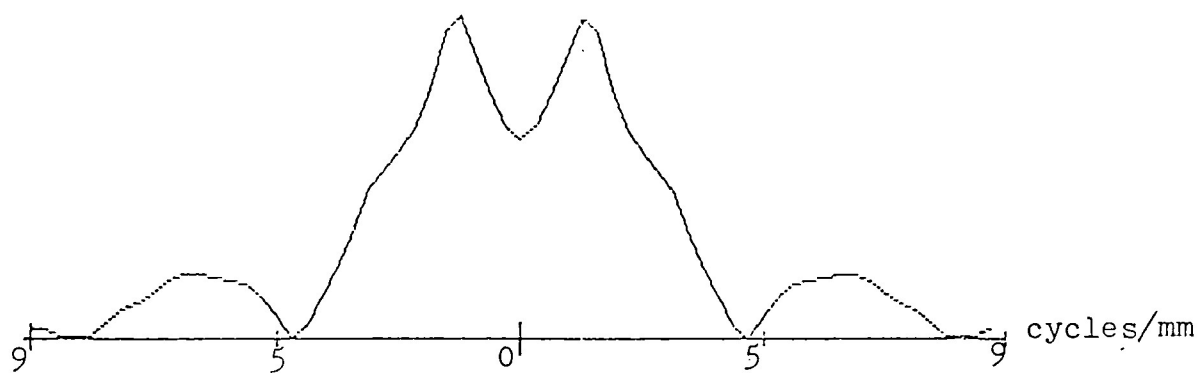


Figure 73. MTF for $a = 270\mu\text{m}$, $b = 810\mu\text{m}$.

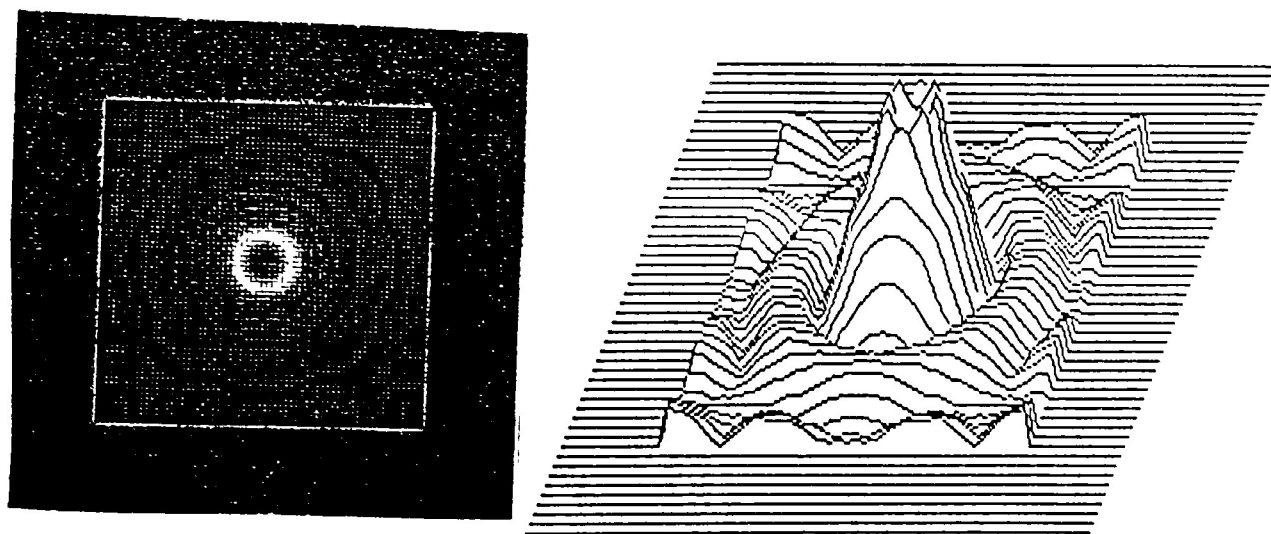


Figure 74. Halftone and Isometric for $a = 270\mu\text{m}$, $b = 810\mu\text{m}$.

APPENDIX F

Digitization Theory¹

Sampling Theory

Sampling theory is applied when a continuously varying analog signal needs to be converted into a digital form. The analog signal will be sampled as shown in Figures 75 and 76.

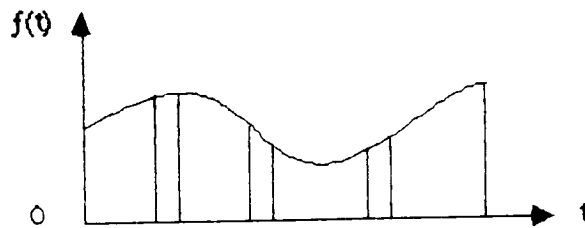


Figure 75. Analog Input Signal

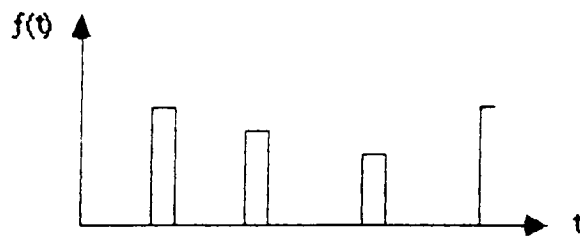


Figure 76. Sampled Waveform

The assumption is made that the signal is band limited (i.e. no frequencies beyond the a

certain cutoff frequency B). This assumption does not introduce significant error into the system. The Fourier Transform of the sampled signal is shown in Figure 77.

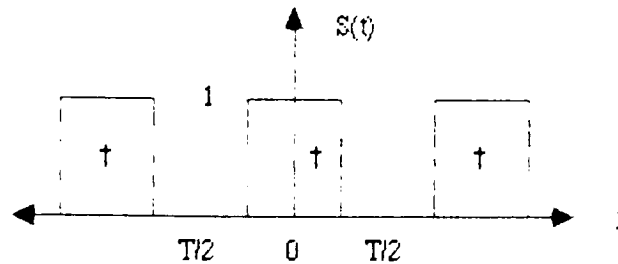


Figure 77. Fourier Transform of $f(t)$

The sampling must be performed at a minimum rate of $f_c \leq 2B$, or signal integrity will be lost. This frequency (f_c) is known as the Nyquist frequency.

The following steps will prove the Nyquist frequency is an accurate assumption for a band limited signal. A sampled signal function $f_s(t)$ can be represented in terms of $f(t)$ by the following relationship. Figure 78 shows the square input wave pulse.

$$f_s(t) = f(t)S(t)$$

$$S(t) = \text{periodic series of pulses}$$

$$\tau = \text{pulse width}$$

$$T = 1/f_c = \text{period}$$

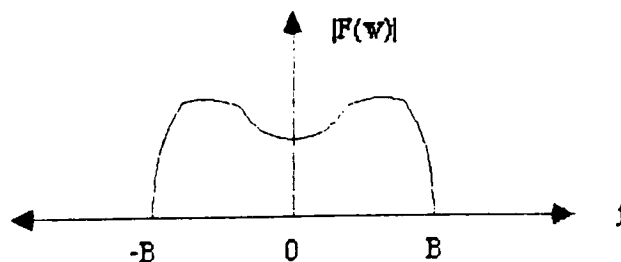


Figure 78. Periodic Switching Function

The function $f_s(t)$ can be described in the following form using a function which contains both a summation of sines and cosines to define the square input pulse wave $S(t)$.

$$f_s(t) = d f(t) \left[1 + 2 \sum_{n=-1}^{\alpha} \frac{\sin(n\pi d)}{n\pi d} \cos(2\pi f_c n t) \right]$$

$$d = \tau/T = \text{duty cycle}$$

The Fourier transform of $f_s(t)$ is represented by the shifting theorem result $F_c(w) = F(w)$, which shifts the output by nw_c where $w_c = 2\pi f_c$.

$$F_c(w) = 1/2 F(w - nw_c) + 1/2 F(w + nw_c)$$

This function is now centered at $\pm nw_c$. The modulation of $\cos nw_c t$ (carrier frequency) results in the function being centered about the carrier. The summation of each value weighted by the $f_s(t)$ function provides the transform of $f_s(t)$, which is shown in the Systems Characterization chapter.

$$\mathcal{F}_s\{S(t)\} = d F(\omega) + d \sum_{n=-\alpha}^{\alpha} \frac{\sin(n\pi d)}{n\pi d} F(\omega - n\omega_c)$$

The sum of the transforms results in the amplitude of each successive component decreasing as $(\sin n\pi d)/n\pi d$. The sampling has effectively shifted the spectrum up to all harmonics of the sampling frequency. This effect is shown in Figure 79.

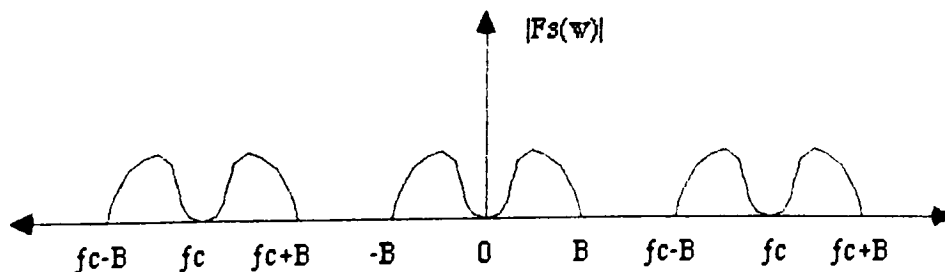


Figure 79. Amplitude Spectrum of a Sampled Input

The signal $f(t)$ can be filtered from $f_s(t)$, as long as the waveforms are separate. If the waveforms overlap the distortion (aliasing) will result in lost signals. The limiting frequency at which $F(w)$ and $F(w-w_c)$ merge, shown in Figure 79, is given by $f_c = 2B$. The Nyquist frequency is critical to the digitization process.

Quantization Theory

Quantization is the process of digitizing the sampled analog signal. It assigns a predetermined binary number to each signal level. This process results in the irretrievable loss of data (rounding error). This result limits the ability to distinguish fine gradations of the analog signal. The electronic noise in the system is reduced, which increases the quality of the signal reproduction. This noise level is reduced further by having a high number of binary levels, which is a feature the scanner applies by using 256 gray levels. This number of levels increases the bandwidth of the system, but this is not a problem in this application.

FOOTNOTES

¹Schwartz, Misha, Information, Transmission, Modulation and Noise. New York: McGraw-Hill Book Company, 1980: 92-96.